Lattice Quantum Chromodynamics Spectroscopy

Monte Carlo Searches For Exotic Charmonium Meson States

David-Alexander Robinson Sch.
08332461

The School of Mathematics, The University of Dublin Trinity College

16th March 2012

Contents

Abstract

In this study the exotic charmonium mesonic states of lattice Quantum Chromodynamics were investigated. Quantum Chromodynamics and lattice Quantum Chromodynamics were reviewed. The $\mathcal{L}$agrangians of these theories and their associated mechanics were discussed. It was found that the non-Abelian nature of Quantum Chromodynamics gives rise to challenging equations. Non-perturbative analysis of these requires computational simulation of the theory on a four dimensional Euclidean lattice. The simple quark model and bound quark-antiquark states were reviewed. Moreover exotic quark-antiquark states were reviewed, including those of purely gluonic states know as glueball states.

The Path Integral Formalism of quantum field theory was derived and using it the correlation function for a free scalar quantum field theory on a periodic lattice was calculated analytically. It was found that the correlation function decays exponentially in time with the hyperbolic-sine of the mass of the state.

Variational fitting was done to Monte Carlo generated data and a mass was extracted using a chi-squared test for an allowed mesonic state and an exotic mesonic state. It was found that the 1^{--} state had a mass of $3.04499 \pm 0.0004\,\mathrm{GeV}$ while the 1^{-+} exotic state had a mass of $4.211 \pm 0.011\,\mathrm{GeV}$.

The partial differential Schrödinger equation was solved by the method of separation of variables for the radial wavefunction $R(r)$. C++ code was written to solve the radial wavefunction equation using the Numerov three-point algorithm for a range of potential functions, including the Cornell Potential and that of the gluon-flux tube. Graphs of the radial wavefunctions were plotted for a range of energy levels n and angular momentum quantum numbers l. In addition the spectrum of the $c\bar{c}$ mesonic states was plotted.

Acknowledgements

Dr. Mike J. Peardon[†] to whom I am indebted for his consistent guidance, encouragement and help. His enthusiasm led me to enjoy every moment of this project.

Sr. Pol Vilaseca Marinar[‡], Mr. Graham Moir[§] and Mr. Tim Harris Sch.[§] for their stylish education in the art of quantum field theory.

Mr. Pádraig Ó Conbhuí[¶] and Mr. Cian Booth[¶] for continual help and countless debugging.

And all of the Lattice Quantum Chromodynamics undergraduate students.

[†]Trinlat Lattice Quantum Chromodynamics Collaboration, The School of Mathematics, The University of Dublin Trinity College

[‡]Graduate Student, The School of Mathematics, The University of Dublin Trinity College, from whom the cover illustration is adapted with kind permission

[§]Graduate Student, The School of Mathematics, The University of Dublin Trinity College

[¶]Theoretical Physics, The School of Mathematics, The University of Dublin Trinity College

Chapter 1

Introduction & Theory

1.1 The Path to Quantum Chromodynamics

Our universe is governed by four fundamental forces, which, in order of elucidation are the *Gravitational Force*, the *Electromagnetic Force*, the *Weak Interactions*, and the *Strong Interactions*. The gravitational and electromagnetic forces are long range, and permeate our lives. Thus we are most familiar with them. The gravitational force was first put on firm footing by Newton in 1678[1], and brought into its modern relativistic formulation by Einstein in the 1910s[2, 3, 4]. In contrast, the weak and strong interactions act only on a distance scale of $\simeq 10^{-15}$m.

The weak interactions, or *Weak Nuclear Force* only reveals itself in nuclear physics, through the guise of nuclear beta decay. First observed in 1896 by Becquerel, it was not fully appreciated as an independent force until the *Fermi Model of The Weak Interaction* in 1933[5]. The weak force culminated in the *Electroweak Unification*. Described first by Glashow in 1961[6], and then modelled as a spontaneously broken gauge theory by Weinberg and Salam in 1967[7, 8], the so called *Glashow-Weinberg-Salam Model* was shown to be a renormalisable quantum field theory by t'Hooft in 1971[9].

Thus the strong force remained to be described. The first categorical effort to describe the then known spectrum of mesons and baryons was the *Eightfold Way* of Gell-Mann in 1961[10]. This was to the elementary particles what the periodic table of Mendeleev was to the chemical elements, arranging the mesons

and baryons into multiplets, namely the spin-1/2 baryon octet, the pseudoscalar meson octet and the spin-3/2 baryon decuplet. Following this, in 1964 Gell-Mann and Zweig independently suggested that the hadrons were composed of fundamental particles, called *quarks*[11, 12]. At this time there were only three flavours of quarks proposed. However, the 1974 coinciding discovery of the ψ particle at Brookhaven by Ting and the J particle at Stanford by Richter in the so-called *November Revolution* introduced a fourth flavour of quark[13, 14]. These two particles were in fact one and the same thing, however the disagreement in naming it led to it baring both names as the J/ψ particle. This fourth quark flavour had in fact been proposed four years earlier in 1970 by Glashow, Iliopoulos and Maiani to resolve a discrepancy in the calculated decay rate of neutral K mesons with that of the experimentally measured rate[15].

At this time, the quark model was not readily accepted, but rather the fine structure of the nucleons were described in terms of partons, as per Feynman's model[16]. It was not until deep inelastic scattering experiments at Stanford in 1968 showed that indeed the nucleons contained point-like scattering centres[17]. This led to the acceptance of the quark model, paving the way for the gauge theory of Quantum Chromodynamics.

1.2 Quantum Chromodynamics

The *Simple Quark Model*[18] aims to predict the hadronic states as the combination of six quarks, the u, d, s, c, b and t quarks, or the *Up*, *Down*, *Strange*, *Charm*, *Beauty* and *Truth* quarks respectively. In this model the hadrons are classed as either *Mesons*, composed of one quark and one antiquark $q\bar{q}$, or *Baryons*, composed of three quarks (qqq) or three antiquarks ($\bar{q}\bar{q}\bar{q}$). Thus the quarks must have a baryon number of 1/3 as well as an electric charge in multiples of $\pm 1/3$.

Quantum Chromodynamics, a non-Abelian gauge theory[19], goes beyond this simple quark model. According to Quantum Chromodynamics there exists another quantum number which the quarks and antiquarks possess, the *Colour Charge*[20, 21], denoted by *Red*, *Green* and *Blue* or *Anti-Red*, *Anti-Green* and *Anti-Blue* respectively. This colour force is flavour blind such that it acts equally on all flavours of quark. Moreover, as per Quantum Chromodynamics,

the colour force is described as being mediated by massless spin-1 vector gauge bosons, called *Gluons*. Due to the non-Abelian nature of Quantum Chromodynamics, these gluons also possess colour charge, whence they participate in self-interactions.

In 1973 it was found by Politzer[22], Gross and Wilczek[23] that the dynamics of Quantum Chromodynamics predicted a scaling behaviour referred to as *Asymptotic Freedom*[24], whereby the strength of the strong interactions decreases with increasing energy. This was attributed to the non-Abelian nature of Quantum Chromodynamics, and the gluonic self-interactions that come with this property. In addition, it was seen that non-Abelian gauge theories are the only class of quantum field theory which display this asymptotic freedom[25], cementing the place of Quantum Chromodynamics as the theory of the strong interactions.

1.3 The Quantum Chromodynamics $\mathcal{L}$agrangian

Quantum Chromodynamics is described by the $SU(3)$-colour $\mathcal{L}$ie group[26], which is non-Abelian. This has $\mathcal{L}$ie bracket commutation relations

$$[T_a, T_b] = i f_{abc} T^c \tag{1.1}$$

where the T_i are the *Generators* of the associated $\mathcal{L}$ie algebra and the f_{abc} are the *Structure Constants*. Now, there are two fundamental degrees of freedom, the fermionic matter fields, and the bosonic gauge fields. The $\mathcal{L}$agrangian is then

$$\mathcal{L} = \sum_{a=1}^{6} \left[\frac{1}{2} i \bar{q}^a(x) \gamma^\mu \overleftrightarrow{D}_\mu q^a(x) - m_a \bar{q}^a(x) q^a(x) \right] - \frac{1}{4} G^a_{\mu\nu} G^{\mu\nu a} \tag{1.2}$$

where the sum over a is the sum over the quark flavours u, d, s, c, b and t, and the

$$G^a_{\mu\nu} = \partial_\mu B^a_\nu(x) - \partial_\nu B^a_\mu(x) + g f_{abc} B^b_\mu(x) B^c_\nu(x) \tag{1.3}$$

are the *Chromomagnetic Field Strength Tensors* and the $B_\mu(x)$ are the *Chromomagnetic Field Potentials*. Furthermore, $\overleftrightarrow{D}_\mu$ is the *Covariant Derivative*

$$D_\mu = \partial_\mu I - \frac{1}{2} i g \lambda^a B^a_\mu \tag{1.4}$$

with the λ^a being the $\mathcal{H}$ermitian, traceless *Gell-Mann Matrices* given by

$$\lambda_1 = \begin{pmatrix} 0 & 1 & 0 \\ 1 & 0 & 0 \\ 0 & 0 & 0 \end{pmatrix}, \quad \lambda_2 = \begin{pmatrix} 0 & -i & 0 \\ i & 0 & 0 \\ 0 & 0 & 0 \end{pmatrix}, \quad \lambda_3 = \begin{pmatrix} 1 & 0 & 0 \\ 0 & -1 & 0 \\ 0 & 0 & 0 \end{pmatrix},$$
$$\lambda_4 = \begin{pmatrix} 0 & 0 & 1 \\ 0 & 0 & 0 \\ 1 & 0 & 0 \end{pmatrix}, \quad \lambda_5 = \begin{pmatrix} 0 & 0 & -i \\ 0 & 0 & 0 \\ i & 0 & 0 \end{pmatrix}, \quad \lambda_6 = \begin{pmatrix} 0 & 0 & 0 \\ 0 & 0 & 1 \\ 0 & 1 & 0 \end{pmatrix},$$
$$\lambda_7 = \begin{pmatrix} 0 & 0 & 0 \\ 0 & 0 & -i \\ 0 & i & 0 \end{pmatrix}, \quad \lambda_8 = \frac{1}{\sqrt{3}} \begin{pmatrix} 1 & 0 & 0 \\ 0 & 1 & 0 \\ 0 & 0 & -2 \end{pmatrix} \tag{1.5}$$

These are twice the generators such that

$$T^a = \frac{\lambda^a}{2} \tag{1.6}$$

Finally, g is the *Coupling Constant*.

1.4 Lattice Quantum Chromodynamics

Owing in part to the non-Abelian nature of Quantum Chromodynamics, in its early years only perturbative calculations were possible. However the lattice formulation of Quantum Chromodynamics by Wilson in 1974[27] allowed research to enter the non-perturbative regime using computational methods. *Lattice Quantum Chromodynamics* was developed to help explain asymptotic freedom without the need for gauge fixing[28]. Indeed, using an expansion to lowest order in the inverse coupling constant Wilson was able to show confinement in strongly coupled lattice Quantum Chromodynamics[27].

So called *Lattice Gauge Theories* define Quantum Chromodynamics mathematically, and thus allow for the simulation of any system. However, the limitations of computational expense must be taken into account. To compute matrix elements, the system must be transformed to Euclidean time, and the Green functions calculated. Finally, the continuum limit must be taken as part of the renormalisation approach[29, 30].

Unfortunately problems arise when Quantum Chromodynamics is considered on a lattice. The foremost of these is the problem of *Fermion Doubling*. Here, fermionic fields on the lattice introduce extra contributions to correlation function integrals, namely 2^d contributions for a d-dimensional system, when in the continuum limit all but one of these should vanish. This has its origins in the use of symmetric lattice derivatives which respect hermiticity, locality and translational invariance as per Nielson[31].

This leads to the introduction of the *Wilson Action*[32] for so-called Wilson fermions in order to eliminate the fermion doubling problem. Yet again this introduces new problems though, as these Wilson fermions break chiral symmetry. This is the symmetry whereby left-handed and right-handed fermions transform independently under rotations in two dimensions.

In response to this undesired broken symmetry, the method of *Staggered Fermions* was introduced by Susskind and Kogut[33, 34, 35]. These staggered fermions correspond to fermions which have an effective lattice spacing of twice that of the fundamental lattice spacing. This works to eliminate the unwanted doubled fermions. Once again, this approach brings its own problems, here making for complicated construction of the quantum fields that are to populate the lattice[36]. It is this staggered approach to lattice Quantum Chromodynamics calculations that dominates.

Once a lattice approach has been chosen, and the required calculation set up, *Monte Carlo Simulations* are used to approximately calculate the path integral. For this, a state is generated randomly from the set of possible states, and the integral approximated. This process is then repeated for a large number of steps N, and the results summed. On completion of the sampling the result is renormalised with respect to the number of steps. This method however introduces new statistical errors to the calculation, due to the probabilistic nature

of the Monte Carlo method random sampling. This can be reduced by a factor of $1/\sqrt{N}$ by taking a large number of steps, however this again increases the computational expense of a calculation. These errors are compounded by the so-called systematic errors which arise due to the finite lattice spacing, and also the finite volume of space over which the calculation is performed.

Another error is introduced in the form of the *Quenched Approximation*, also known as the valence quark approximation, first used by Weingarten and Parisi in 1981[37, 38]. This approximation amounts to neglecting the virtual quark-antiquark pairs and gluons which may be created at any moment on the lattice. That is, it neglects the quark sea, and considers only the interactions of the valence quarks. This has the benefit of greatly speeding up calculation times. Moreover, it can give results within about 10% of the accepted values, as the hardonic spectrum calculations of the Japanese CP-PACS collaboration showed in 1998[39].

Modern calculations may be performed using 'full Quantum Chromodynamics', moving beyond the quenched approximation, thanks to increasingly powerful computers and innovative algorithms. Such machines as those of the QCDSP at the RIKEN Brookhaven Research Centre and at Columbia University[40], and the UKQCD machine at the University of Edinburgh[41] are capable of performing billions of floating point operations per second on heavily parallelised computers.

These collaborations have been able to calculate increasingly accurate spectra of the hadrons. Furthermore, the calculation of exotic mesons such as those predicted by the Gluon-Flux Tube Model are made possible, as well as those of so-called *Glueballs*. It has in fact been found that recent glueball masses simulated with $(2 + 1)$flavours of sea quarks[42], namely the strange quark and small mass up and down quarks, show negligible changes to the mass predicted by those calculations without sea quarks[43]. Currently the lightest predicted scalar glueball is know as the $f_j(1710)$ particle[44].

1.5 The Lattice Quantum Chromodynamics $\mathcal{L}$agrangian

At its core, lattice Quantum Chromodynamics is a non-perturbative method to evaluate the path integral of Quantum Chromodynamics, by considering a system of quarks and gluons on a grid of space-time points, namely with quarks on the lattice sites and gluons in the lattice spacings, referred to here as *Links*. For a grid of lattice spacing a we have an automatic momentum cut-off of order$1/a$ called the *Regulator*. Hence lattice Quantum Chromodynamics is a mathematically well defined quantum field theory, in the sense that it is renormalisable.

To go from a quantum field theory to a lattice quantum field theory one must perform a *Wick Rotation* of space-time to a Euclidean lattice $t \to i\tau$ and then discretise the Euclidean action S_E in such a way as to regain the physical space-time action as $a \to 0$.

From the action for fermions

$$S_F(\psi, \bar{\psi}, A) = \sum_{f=1}^{n_f} \int d^4x \, \bar{\psi}^f(x)(\not{D} + m_f)\psi^f(x) \tag{1.7}$$

where n_f is the number of quark flavours, the derivative is a finite differential operator which may be discretised as

$$\partial_\mu \psi(x) = \frac{1}{2a}\left[\psi(n+\mu) - \psi(n-\mu)\right] \tag{1.8}$$

giving

$$S_F^{latt}(\psi, \bar{\psi}) = a^4 \sum_{n\in\Lambda} \bar{\psi}(n) \left(\sum_{\mu=1}^{4} \frac{\gamma^\mu}{2a}\left[\psi(n+\hat{\mu}) - \psi(n-\hat{\mu}) + m\psi(n)\right] \right) \tag{1.9}$$

which describes free fermions.

The *Link Matrices* U_μ with $U_\mu \in SU(3)$ are defined by

$$U_\mu = \exp(iaA_\mu) \tag{1.10}$$

with

$$U_{-\mu}(n) \equiv U_{\mu}^{\dagger}(n-\hat{\mu}) \tag{1.11}$$

Therefore

$$S_F^{latt}(\psi,\bar{\psi}) = a^4 \sum_{n\in\Lambda} \bar{\psi}(n) \left[\sum_{\mu=1}^{4} \left(\frac{U_\mu(n)\psi(n+\hat{\mu})}{2a} - \frac{U_{-\mu}(n)\psi(n-\hat{\mu})}{2a} + m\psi(n) \right) \right] \tag{1.12}$$

and this is the *Lattice Action for Fermions*. Here there are fermions in a background gauge field such that the fermions interact with the gluons, but there are no gluonic self-interactions.

1.6 The Path Integral Formalism

The time evolution of a quantum mechanical system is given by the Schrödinger equation

$$|\psi(t)> = \exp\left(-i\mathcal{H}(t-t_0)\right)|\psi(t_0)> \tag{1.13}$$

where $\mathcal{H}$ is the Hamiltonian of the system.

For a classical system, the time evolution is given by Lagrange's equations of motion, which may be found by taking a variation in the action of the system and then using $\mathcal{H}$amilton's principle of least action. To proceed to a quantum system the equations of motion are written in terms of the Hamiltonian and the Poisson brackets. Then by the process of canonical quantisation a quantum mechanical system is obtained.

Here the Poisson bracket is promoted to the Commutator

$$\{.,.\} \to [.,.] \tag{1.14}$$

and the canonical commutation relations are defined as

$$[\phi(\vec{x},t),\phi(\vec{y},t)] = 0 \tag{1.15}$$

$$[\phi(\vec{x},t),\pi(\vec{y},t)] = i\delta^{(3)}(\vec{x}-\vec{y}) \tag{1.16}$$

with the former preserving causality, and the latter mimicking the quantum mechanical commutator.

However, in this method the original principle of least action has been lost. As per Feynman[45], a representation for the Green function may be derived, such that the connection to the principle of least action is retained.

Considering the Heisenberg picture of quantum mechanics, in which operators are time dependent such that

$$Q(t) = \exp(i\mathcal{H}t)Q\exp(-i\mathcal{H}t) \tag{1.17}$$

with instantaneous eigenstates

$$|q,t> = \exp(i\mathcal{H}t)|q> \tag{1.18}$$

giving

$$\begin{aligned} Q(t)|q,t> &= \exp(i\mathcal{H}t)Q\exp(-i\mathcal{H}t)\exp(i\mathcal{H}t)|q> \\ &= q|q,t> \end{aligned} \tag{1.19}$$

Thus

$$< q'',t''|q',t' > = < q''|\exp[-i\mathcal{H}(t''-t')]|q' >$$

or

$$< q'',t''|q',t' > = < q''|\exp[-i\mathcal{H}(N+1)\varepsilon]|q' > \tag{1.20}$$

with

$$t''-t' = (N+1)\varepsilon$$

Inserting a complete set of eigenstates with

$$\int_{-\infty}^{\infty} \mathrm{d}q\, |q>< q| = 1$$

yields

$$< q'',t''|q',t' > = \int_{-\infty}^{\infty} \prod_{j=1}^{N} \mathrm{d}q_j \; < q''|\exp(-i\mathcal{H}\varepsilon)|q_N >< q_N|\exp(-i\mathcal{H}\varepsilon)|q_{N-1} >< q_{N-1}|\times\ldots$$
$$\cdots \times |q_1 >< q_1|\exp(-i\mathcal{H}\varepsilon)|q' >$$

In general

$$\exp(A)\exp(B) \neq \exp(A+B)$$

for $[A,B] \neq 0$. But by Baker-Cambell-Hausdorff

$$\exp[\lambda(A+B)] \simeq \exp(\lambda A)\exp(\lambda B)\exp(1/2\lambda^2[A,B])\ldots \tag{1.21}$$

or for $\varepsilon \ll 1$

$$\exp(-i\mathcal{H}\varepsilon) \simeq \exp(-iP^2\varepsilon/2m)\exp(-iV(Q)\varepsilon) \tag{1.22}$$

where

$$\mathcal{H} = \frac{P^2}{2m} + V(Q) \tag{1.23}$$

This gives

$$\begin{aligned} < q_{j+1}|\exp(-i\mathcal{H}\varepsilon)|q_j > &= \int_\infty^\infty \mathrm{d}p_1 < q_{j+1}|\exp(-iP^2\varepsilon/2m)|p_1 >< p_1|\exp(-iV(Q)\varepsilon)|q_j > \\ &= \int_\infty^\infty \mathrm{d}p_1 \exp(-iP^2\varepsilon/2m)\exp(-iV(Q)\varepsilon) < q_{j+1}|p_1 >< p_1|q_j > \\ &= \int_\infty^\infty \frac{\mathrm{d}p_1}{2\pi}\exp(-iP^2\varepsilon/2m)\exp(-iV(Q)\varepsilon)\exp(ip_1q_{j+1})\exp(-ip_1q_j) \\ &= \int_\infty^\infty \frac{\mathrm{d}p_1}{2\pi}\exp[-i\mathcal{H}(p_1,q_j)\varepsilon]\exp[ip_1(q_{j+1}-q_j)] \end{aligned} \tag{1.24}$$

So letting $q_0 = q'$ and $q_{N+1} = q''$ yields

$$< q'', t''|q', t' >= \int_{-\infty}^{\infty} \prod_{k,j=0}^{N+1} \frac{\mathrm{d}q_k \mathrm{d}p_j}{2\pi} \exp[-i\mathcal{H}(p_j,q_j)\varepsilon]\exp[ip_j(q_{j+1}-q_j)] \tag{1.25}$$

Then taking the limit as $\varepsilon \to 0$ and $N \to \infty$ gives

$$\lim_{\substack{\varepsilon\to 0 \\ N\to\infty}} < q'', t''|q', t' >= \int_{-\infty}^{\infty} \mathscr{D}p\,\mathscr{D}q\,\exp\left[i\int_{t'}^{t''} \mathrm{d}t(p\dot{q} - \mathcal{H})\right] \tag{1.26}$$

where

$$\mathscr{D}p = \prod_{k=0}^{N+1} \frac{\mathrm{d}p_k}{\sqrt{2\pi}} \qquad \text{and} \qquad \mathscr{D}q = \prod_{j=0}^{N+1} \frac{\mathrm{d}q_j}{\sqrt{2\pi}}$$

Here $\mathcal{H}$ is *Weyl Ordered* such that it does not contain terms or the form p^iq^j. Moreover, it is quadratic in p, and so taking the *Stationary Phase* is equivalent

to computing the integral explicitly. Thus

$$\frac{\partial}{\partial p}\left(i\int_{t'}^{t''}\mathrm{d}t(p\dot{q}-\mathcal{H})\right)=0$$

whence

$$\dot{q}=\frac{\partial\mathcal{H}}{\partial p} \tag{1.27}$$

Hence solving for $p=p(\dot{q})$ and substituting in for $\mathcal{H}$ removes the need to integrate over $\mathscr{D}p$. Moreover, since $p\dot{q}-\mathcal{H}$ is the reverse of a $\mathcal{L}$egendre Transformation this yields

$$<q'',t''|q',t'>=\int_{-\infty}^{\infty}\mathscr{D}q\,\exp\left[i\int_{t'}^{t''}\mathrm{d}t\mathcal{L}(q,\dot{q})\right] \tag{1.28}$$

and this is the desired *Path Integral*.

1.7 Bound Quark-Antiquark Mesons

In the quark model a bound state of any quark and its corresponding antiquark is allowed. These particles are mesons known as *Quarkonia*. The light quarks, the u, d, and s, are relativistic, and thus the Schrödinger equation is not applicable, their study requiring a quantum field theoretic approach. The heavy mesons on the other hand, that is the c, b, and t, may be analysed in the non-relativistic regime. However the strong interactions are much more complicated than that of the electromagnetic force with governs the Hydrogen atom, say, and so an analytic solution is not attainable.

At short distances, due to asymptotic freedom, it is expected that the strong interactions have a Coulombic

$$V(r)\propto\frac{1}{r}$$

potential. Moreover, a fine structure behaviour similar to that of positronium is expected[46, 47]. At large ranges however the confinement behaviour of quarks takes over, and the model breaks down.

Before the discovery of the J/ψ particle (see 1.1), Appelquist and Politzer[48, 49] predicted that the charm quark should behave non-relativistically, and thus

that it should form bound states $c\bar{c}$. After the discovery of the J/ψ particle, many other energy states of bound $c\bar{c}$ quarks were found[50]. These are the spin-0 singlet state η_c, the spin-1 triplet states ψ, ψ', ψ'' and ψ''' and the P-wave states χ_{c0}, χ_{c1} and χ_{c2}. Here the successive dashes correspond to successively higher energy levels of the ψ particle. The energy spectrum of these states was even found be similar to that of positronium.

Those $c\bar{c}$ states for energy levels $n = 1, 2$ are relatively long lived with lifetimes of the order $\simeq 10^{-20}$. This is because they are both below the threshold for D meson production, as well as the fact that the Okubo-Zweig-Iizuka rule[51, 52, 53, 54] suppresses their strong decay. This is because the gluons involved in the decay

$$c\bar{c} \to u\bar{d} + d\bar{d} + d\bar{u}$$

corresponding to a $c\bar{c}$ particle decaying into three pions are high energy 'hard' gluons, and thus they couple weakly due to asymptotic freedom.

However, for energy levels above $n = 3$ the production of D mesons becomes possible, and the $c\bar{c}$ particles have shortened lifetimes. These quasi-bound $c\bar{c}$ states have been observed for energy levels up to $n = 5$.

In addition, bound states of two beauty quarks are possible. Again, before the discovery of the b quark, Eichten and Gottfried[55] predicted the existence of such bound states in 1976. One year later the Υ meson was discovered. Since then, spin-1 states up to $n = 6$ have been observed, as well as P-wave states for $n = 2$ and $n = 3$.

Due to the large mass of the beauty quark, b and $\bar{b}$ quark pairs form three energy levels of bound states. Despite this however, the $b\bar{b}$ spectrum is again similar to that of the $c\bar{c}$[56].

Recent construction of B-factories[57] in the search for CP violation in the decay of B mesons as suggested by Carter and Sanda in 1981[58] has led to renewed study of $c\bar{c}$ mesons with greatly improved statistics, as they are produced en mass at these facilities.

Unlike the charm and beauty quarks, there does not exist bound states $t\bar{t}$ of the truth quark. This is because it is too massive, and therefore its lifetime too short to form bound states.

1.8 Allowed Quarkonium Quantum States

For a quarkonium meson, composed of a bound state of two spin-1/2 fermions, the allowed *Total Spin* states are $S = 0, 1$ for the spin-singlet and spin-triplet respectively. Then, for a meson with orbital angular momentum L the *Total Angular Momentum* J is given by

$$\vec{J} = \vec{L} + \vec{S} \tag{1.29}$$

Atomic spectroscopic notation may be used to denote an excitation state of a particle as J^{PC}, where P and C are the particles *Parity* and *Charge Conjugation* quantum numbers respectively, given for a bound state of a quark-antiquark pair by[59]

$$P = (-1)^{L+1} \quad \text{and} \quad C = (-1)^{L+S} \tag{1.30}$$

Now, for a quarkonium meson in the ground state with $L = 0$ the allowed total angular momentum is $J = 0, 1$ for total spin states $S = 0, 1$ respectively, and so the allowed quantum states are $J^{PC} = 0^{-+}, 1^{--}$. These are both s-wave states and correspond to the η_c and J/ψ particles respectively.

For P-wave states with $L = 1$ the allowed total angular momentum is $J = 1$ or $J = 0, 1, 2$ for total spin states $S = 0, 1$ respectively, and so here the allowed quantum states are $J^{PC} = 1^{+-}$ for the spin-singlet and $J^{PC} = 0^{++}, 1^{++}, 2^{++}$ for the spin-triplet.

Moreover, for a quarkonium meson with $L = 2$ the allowed total angular momentum is $J = 2$ or $J = 1, 2, 3$ for total spin states $S = 0, 1$ respectively, whence the allowed quantum states are $J^{PC} = 2^{-+}$ and $J^{PC} = 1^{--}, 2^{--}, 3^{--}$. These states are D-wave.

Finally, for F-wave states with $L = 3$ the allowed total angular momentum is $J = 3$ or $J = 2, 3, 4$ for total spin states $S = 0, 1$ respectively, giving allowed quantum states $J^{PC} = 3^{+-}$ and $J^{PC} = 2^{++}, 3^{++}, 4^{++}$.

Thence it is seen that the allowed quantum states are

$$\begin{array}{cccc} 0^{-+}, & & 2^{-+}, & \cdots \\ & 1^{--}, & 2^{--}, & 3^{--}, \cdots \\ 0^{++}, & 1^{++}, & 2^{++}, & 3^{++}, \cdots \\ & 1^{+-}, & & 3^{+-}, \cdots \end{array} \tag{1.31}$$

and so on.

1.9 Exotic Charmonium Quantum States

From the above it is clear that for a bound state of a quark-antiquark pair not all quantum states are allowed. Namely, those states J^{+-} for J even and J^{-+} for J odd. Moreover, the 0^{--} and 0^{+-} states are not allowed. These states are known as *Exotic States*.

However, there has been some experimental evidence to suggest the existence of such exotic charmonium states. The first of these exotic charmonium like states was discovered by the Bell collaboration in 2003[60] when an unlikely conventional charmonium candidate was found with a mass spectrum near 3872 MeV through the decay

$$B^+ \to K^+ + \pi^+ + \pi^- + J/\psi$$

which came to be known as the $X(3872)$ meson. This discovery was later confirmed by the BABAR team[61] and also in $p\bar{p}$ collisions at the Tevatron by both the CDF[62, 63, 64] and DØ[65]. Furthermore, decays of the X to a D^{*0} and a $\bar{D}^0$ pair were seen by both the BABAR[66] and Bell[67] collaborations.

In addition, vector charmonium-like states have been detected by the BABAR team as early as 2005[68], which became known as the $Y(4260)$ meson. This was again seen by the BABAR collaboration in 2008[69], as well as by the CLEO[70] and Belle[71] teams afterwards, in 2006 and 2007 respectively. What is more, in 2007 the BABAR team found another state at 4360 MeV[72], which they called the $Y(4360)$ meson. Once again, this state was later found by the Belle collaboration[73].

Finally, some charmonium-like charged mesons have been found, which are known as Z states, first seen by Belle in 2008[74], and have a minimal quark substructure of $c\bar{c}u\bar{d}$. Thus they are manifestly exotic[75].

The first hints of the quark-sea came from deep inelastic scattering experiments at Stanford in the late 1960s. They measured proton structure functions, which describe the distribution of the proton's momentum, and hence help to describe its internal structure. Later structure function measurements performed at DESY found a distribution of momentum fractions, with few quarks having a large fraction of the proton's momentum. This suggested that there was more than simply three valence quarks each carrying one third of the proton's momentum, but rather a whole 'sea' of gluons, quarks and antiquarks.

The first evidence of antiquarks in the proton were detected at the Gargamelle Bubble Chamber at CERN in 1973. Here neutrinos and antineutrinos were used in deep inelastic scattering experiments with protons. The fact that all neutrinos are left-handed, while all antineutrinos are right-handed[76], due to their parity violating nature, allows for the determination of quark flavour and antiquark sensitivity.

Furthermore, the presence of strange quarks within the nucleon was found by the Chicago-Columbia-Fermilab-Rochester Collaboration in di-muon experiments preformed in 1974[77] at Fermilab. Here, an incoming muon neutrino scattering off a strange quark in the nucleon becomes a muon, while the W^+ boson which interacts with the strange quark creates a charm quark. This charm quark in turn decays to give an anti-muon, and hence the signature of the process is the detection of a pair of muons of opposite sign.

$$\begin{aligned} p + \nu_\mu &\rightarrow \mu^- + c \\ &\hookrightarrow \mu^+ + \nu_\mu + s \end{aligned} \tag{1.32}$$

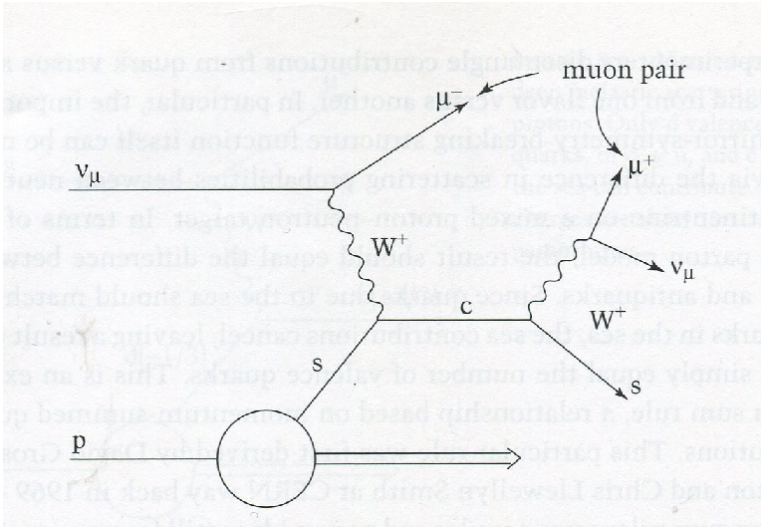

Figure 1.1: Neutrino deep inelastic scattering from a strange sea quark creates a di-muon signature. Adapted from [78] with kind permission, copyright (2004) Cambridge University Press

Following this, in 1996 the upgraded experiment, NuTeV, found evidence of charm quarks inside the proton by the detection of so-called 'wrong-sign' muons. In this experiment a muon neutrino scattering off a charm quark by exchange of a neutral Z^0 boson remains a neutrino. However the charm quark then decays to again give a strange quark, a muon neutrino and an anti-muon.

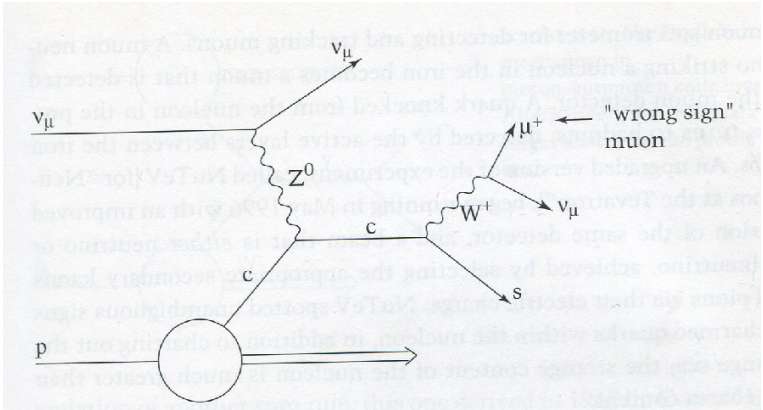

Figure 1.2: Neutrino deep inelastic scattering from a charm sea quark creates an antimuon signature. Adapted from [78] with kind permission, copyright (2004) Cambridge University Press

The explanation of the existence of these states requires a more advanced description, beyond that of the simple quark model.

The *MIT Bag Model* framework, developed by Johnson in 1974[79, 80] may

be used to calculate a large number of interesting quantities and processes. It has effectively been used to calculate the masses of the light hadrons[81], as well as the spectrum of some unconventional hadron states such as $qq\bar{q}\bar{q}$[82] and even pure gluonic states, known as glueballs[83]. Here, the confinement property is reproduced by requiring that the colour current through some surface vanishes, where the colour current is given by

$$J^a_\mu = (\bar{q}_r, \bar{q}_g, \bar{q}_b)\, \lambda^a \gamma_\mu \begin{pmatrix} q_r \\ q_g \\ q_b \end{pmatrix} \tag{1.33}$$

with the subscripts here summing over the three colour charges *red*, *green* and *blue*, and the λ^a are the eight colour-$SU(3)$ Gell-Mann matrices. Then for a normal vector n_μ the boundary condition may be written as

$$n^\mu J^a_\mu = 0 \tag{1.34}$$

for all $a = 1, 2, \ldots, 8$. The quarks are then modelled as being constrained to stay within this bag, inside of which there is a population of freely moving quarks of all and any kind.

1.10 The Gluon Flux-Tube Model

Alternatively, the *Gluon Flux-Tube Model*[84] as introduced by Veneziano in 1968 may be used. Here the self interactions of gluons are taken into account. This gives a spectrum closer to that of full Quantum Chromodynamics, and is thus more populous than that of the simple quark model. This is because, even in the absence of quarks, there remains a non-trivial interacting pure gauge theory which has its own spectrum of states. Namely, the flux-tube model allows the existence of multi-quark states, exotic hadrons, and also decays due to flux-tube breaking.

On the lattice, a flux-tube is a directed element such that the scalar

$$\sum_{a=1}^{8} \vec{E_a}^{\,2}$$

has a definite non-zero eigenvalue, where $\vec{E_a}$ is the colour-electric field. These are the links U_μ in the lattice spaces which join together quarks on the lattice sites to form a gauge-invariant configuration. The excitation of this string can then give rise to unconventional states which are not usually present in the simple quark model. Furthermore, purely gluonic states correspond to closed loops of links.

Thus the colour fields are constrained to strings. This again has its origins in the gluonic self-interactions, and is in contrast to the Abelian case of an electromagnetic field, say, in which the field lines go out in all directions (Fig. 1.3). The flux tube is in fact more like a flux sausage than a string.

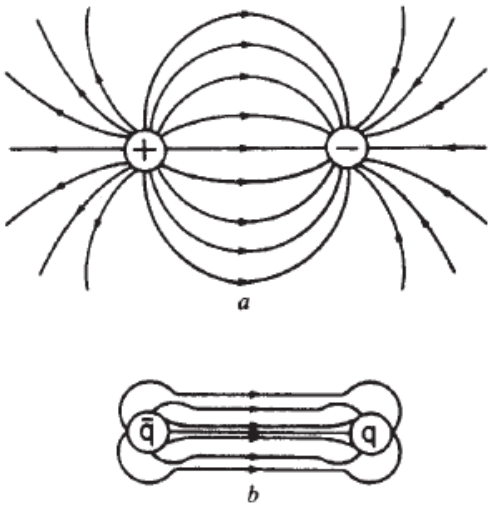

Figure 1.3: (a) electric field lines between a positive and a negative electric charge and (b) colour field lines between a quark and an antiquark. Adapted from [85] with kind permission, copyright (1979) Nature

The *Born-Oppenheimer Approximation* is valid as the gluons move so fast that their effect can be taken as an effective potential. This produces an interaction strength that increases linearly with quark separation, such that the string tension remains constant as the quark-antiquark pair are pulled apart. This

model then reproduces quark confinement, as the energy needed to separate a quark-antiquark pair is infinite.

Moreover, at a large distances, it becomes energetically more favourable to create a quark-antiquark pair out of the vacuum rather than increase the length of the flux tube, leading to two colourless mesons (Fig. 1.4).

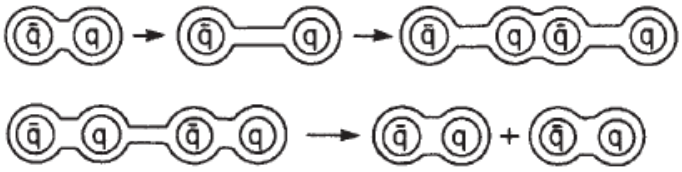

Figure 1.4: As the quarks separate the energy expanded in pulling them apart creates a quark-antiquark pair out of the vacuum resulting in two colourless mesons. Adapted from [85] with kind permission, copyright (1979) Nature

However, this approach is only valid for large-scale Quantum Chromodynamics. As the lattice constant a goes to zero, the flux-tube mixing will become more and more complicated giving rise to very many flux-tube topologies as gluon self-interactions become increasingly important.

Chapter 2

Numerical Calculations of The Radial Wavefunction

2.1 Schrödinger's Equation for The Radial Wavefunction

The Schrödinger Equation is written as

$$\mathcal{H}|\psi> = E|\psi> \tag{2.1}$$

where for a spherically symmetric potential

$$\mathcal{H} = \frac{-\hbar^2}{2m}\vec{\nabla}^2 + V(r) \tag{2.2}$$

and so

$$\left[\frac{-\hbar^2}{2m}\vec{\nabla}^2 + V(r)\right]\psi(\vec{r}) = E\psi(\vec{r}) \tag{2.3}$$

Using the method of separation of variables such that

$$\psi(\vec{r}) = R(r)\Phi(\phi)\Theta(\theta) \tag{2.4}$$

gives

$$\left[\frac{-\hbar^2}{2m}\vec{\nabla}^2 + V(r)\right]R(r)\Phi(\phi)\Theta(\theta) = ER(r)\Phi(\phi)\Theta(\theta) \tag{2.5}$$

Now, in spherical polar coordinates

$$\vec{\nabla}^2 = \frac{1}{r^2}\frac{\partial}{\partial r}\left(r^2\frac{\partial}{\partial r}\right) + \frac{1}{r^2\sin(\phi)}\frac{\partial}{\partial\phi}\left(\sin(\phi)\frac{\partial}{\partial\phi}\right) + \frac{1}{r^2\sin^2(\phi)}\frac{\partial^2}{\partial\theta^2} \tag{2.6}$$

or

$$\vec{\nabla}^2 = \frac{2}{r}\frac{\partial}{\partial r} + \frac{\partial^2}{\partial r^2} + \frac{1}{r^2\tan(\phi)}\frac{\partial}{\partial\phi} + \frac{2}{r^2}\frac{\partial^2}{\partial\phi^2} + \frac{1}{r^2\sin^2(\phi)}\frac{\partial^2}{\partial\theta^2} \tag{2.7}$$

This gives

$$\left\{\frac{-\hbar^2}{2m}\left[\frac{1}{r^2}\frac{\partial}{\partial r}\left(r^2\frac{\partial}{\partial r}\right) + \frac{1}{r^2\sin(\phi)}\frac{\partial}{\partial\phi}\left(\sin(\phi)\frac{\partial}{\partial\phi}\right) + \frac{1}{r^2\sin^2(\phi)}\frac{\partial^2}{\partial\theta^2}\right] + V(r)\right\}R(r)\Phi(\phi)\Theta(\theta) = ER(r)\Phi(\phi)\Theta(\theta)$$

and so

$$\frac{-\hbar^2}{2m}\left[\Phi(\phi)\Theta(\theta)\frac{1}{r^2}\frac{\mathrm{d}}{\mathrm{d}r}\left(r^2\frac{\mathrm{d}}{\mathrm{d}r}\right)R(r) + R(r)\Theta(\theta)\frac{1}{r^2\sin(\phi)}\frac{\mathrm{d}}{\mathrm{d}\phi}\left(\sin(\phi)\frac{\mathrm{d}}{\mathrm{d}\phi}\right)\Phi(\phi) + R(r)\Phi(\phi)\frac{1}{r^2\sin^2(\phi)}\frac{\mathrm{d}^2}{\mathrm{d}\theta^2}\Theta(\theta)\right] + [V(r)-E]R(r)\Phi(\phi)\Theta(\theta) = 0$$

Dividing across by $R(r)\Phi(\phi)\Theta(\theta)\hbar^2/2m$ and subsequently multiplying across by $r^2\sin^2(\phi)$ gives

$$-\frac{\sin^2(\phi)}{R(r)}\frac{\mathrm{d}}{\mathrm{d}r}\left(r^2\frac{\mathrm{d}}{\mathrm{d}r}\right)R(r) - \frac{\sin(\phi)}{\Phi(\phi)}\frac{\mathrm{d}}{\mathrm{d}\phi}\left(\sin(\phi)\frac{\mathrm{d}}{\mathrm{d}\phi}\right)\Phi(\phi) - \frac{1}{\Theta(\theta)}\frac{\mathrm{d}^2}{\mathrm{d}\theta^2}\Theta(\theta) + r^2\sin^2(\phi)\frac{2m}{\hbar^2}[V(r)-E] = 0$$

which is separable such that

$$-\frac{\sin^2(\phi)}{R(r)}\frac{\mathrm{d}}{\mathrm{d}r}\left(r^2\frac{\mathrm{d}}{\mathrm{d}r}\right)R(r) - \frac{\sin(\phi)}{\Phi(\phi)}\frac{\mathrm{d}}{\mathrm{d}\phi}\left(\sin(\phi)\frac{\mathrm{d}}{\mathrm{d}\phi}\right)\Phi(\phi) + r^2\sin^2(\phi)\frac{2m}{\hbar^2}[V(r)-E] = \frac{1}{\Theta(\theta)}\frac{\mathrm{d}^2}{\mathrm{d}\theta^2}\Theta(\theta) \tag{2.8}$$

Here the left hand side is independent of ϕ, while the right hand side is independent of r and θ, and so each is equal to a constant, which may be set as

$-m_l^2$. Then

$$\frac{1}{\Theta(\theta)}\frac{\mathrm{d}^2}{\mathrm{d}\theta^2}\Theta(\theta) = -m_l^2 \tag{2.9}$$

whence

$$\Theta(\theta) = \exp(im_l\theta) \tag{2.10}$$

Furthermore,

$$-\frac{\sin^2(\phi)}{R(r)}\frac{\mathrm{d}}{\mathrm{d}r}\left(r^2\frac{\mathrm{d}}{\mathrm{d}r}\right)R(r) - \frac{\sin(\phi)}{\Phi(\phi)}\frac{\mathrm{d}}{\mathrm{d}\phi}\left(\sin(\phi)\frac{\mathrm{d}}{\mathrm{d}\phi}\right)\Phi(\phi) + \frac{2m}{\hbar^2}r^2\sin^2(\phi)[V(r)-E] = -m_l^2$$

Dividing across by $\sin^2(\phi)$ gives

$$-\frac{1}{R(r)}\frac{\mathrm{d}}{\mathrm{d}r}\left(r^2\frac{\mathrm{d}}{\mathrm{d}r}\right)R(r) - \frac{1}{\sin(\phi)}\frac{1}{\Phi(\phi)}\frac{\mathrm{d}}{\mathrm{d}\phi}\left(\sin(\phi)\frac{\mathrm{d}}{\mathrm{d}\phi}\right)\Phi(\phi) + \frac{2m}{\hbar^2}r^2[V(r)-E] = -\frac{m_l^2}{\sin^2(\phi)}$$

which is again separable such that

$$-\frac{1}{R(r)}\frac{\mathrm{d}}{\mathrm{d}r}\left(r^2\frac{\mathrm{d}}{\mathrm{d}r}\right)R(r) + \frac{2m}{\hbar^2}r^2[V(r)-E] = -\frac{m_l^2}{\sin^2(\phi)} + \frac{1}{\sin(\phi)}\frac{1}{\Phi(\phi)}\frac{\mathrm{d}}{\mathrm{d}\phi}\left(\sin(\phi)\frac{\mathrm{d}}{\mathrm{d}\phi}\right)\Phi(\phi) \tag{2.11}$$

Again, each side is a constant, which can be chosen to be $-l(l+1)$, giving

$$-\frac{1}{R(r)}\frac{\mathrm{d}}{\mathrm{d}r}\left(r^2\frac{\mathrm{d}}{\mathrm{d}r}\right)R(r) + \frac{2m}{\hbar^2}r^2[V(r)-E] = -l(l+1)$$

or on multiplying across by $-R(r)/r^2$

$$\frac{1}{r^2}\frac{\mathrm{d}}{\mathrm{d}r}\left(r^2\frac{\mathrm{d}}{\mathrm{d}r}\right)R(r) - \frac{2m}{\hbar^2}[V(r)-E]R(r) = \frac{l(l+1)}{r^2}R(r)$$

and so

$$\left\{\frac{\hbar^2}{2m}\left[-\frac{1}{r^2}\frac{\mathrm{d}}{\mathrm{d}r}\left(r^2\frac{\mathrm{d}}{\mathrm{d}r}\right) + \frac{l(l+1)}{r^2}\right] + V(r)\right\}R(r) = ER(r) \tag{2.12}$$

or

$$\left\{\frac{\hbar^2}{2m}\left[-\frac{2}{r}\frac{\mathrm{d}}{\mathrm{d}r}-\frac{\mathrm{d}^2}{\mathrm{d}r^2}+\frac{l(l+1)}{r^2}\right]+V(r)\right\}R(r)=ER(r) \tag{2.13}$$

Now, choosing

$$U(r)=rR(r) \tag{2.14}$$

it is seen that

$$\begin{aligned}\frac{\mathrm{d}^2}{\mathrm{d}r^2}\left(U(r)\right)&=\frac{\mathrm{d}^2}{\mathrm{d}r^2}\left(rR(r)\right)\\&=\frac{\mathrm{d}}{\mathrm{d}r}\left(r\frac{\mathrm{d}}{\mathrm{d}r}R(r)+R(r)\right)\\&=r\frac{\mathrm{d}^2}{\mathrm{d}r^2}R(r)+\frac{\mathrm{d}}{\mathrm{d}r}R(r)+\frac{\mathrm{d}}{\mathrm{d}r}R(r)\end{aligned}$$

or

$$-\frac{1}{r}\frac{\mathrm{d}^2}{\mathrm{d}r^2}\left(rR(r)\right)=-\frac{\mathrm{d}^2}{\mathrm{d}r^2}R(r)-\frac{2}{r}\frac{\mathrm{d}}{\mathrm{d}r}R(r) \tag{2.15}$$

Thus equation (2.13) is equivalent to

$$\frac{\hbar^2}{2m}\left[-\frac{1}{r}\frac{\mathrm{d}^2}{\mathrm{d}r^2}\left(rR(r)\right)+\frac{l(l+1)}{r^2}R(r)\right]+V(r)R(r)=ER(r)$$

Multiplying across by r gives

$$\frac{\hbar^2}{2m}\left[-\frac{\mathrm{d}^2}{\mathrm{d}r^2}\left(rR(r)\right)+\frac{l(l+1)}{r^2}\left(rR(r)\right)\right]+V(r)\left(rR(r)\right)=E\left(rR(r)\right)$$

whence it is found that $U(r)$ satisfies

$$\left\{\frac{\hbar^2}{2m}\left[-\frac{\mathrm{d}^2}{\mathrm{d}r^2}+\frac{l(l+1)}{r^2}\right]+V(r)\right\}U(r)=EU(r) \tag{2.16}$$

2.2 Simulations of The Cornell Potential

For the Cornell Potential, given by

$$V(r)=-\frac{\pi}{12r}+\sigma r \tag{2.17}$$

where σ is the string tension with $\sqrt{\sigma} \simeq 400\,\mathrm{MeV}$, equation (2.16) becomes

$$\left\{\frac{\hbar^2}{2m}\left[-\frac{\mathrm{d}^2}{\mathrm{d}r^2}+\frac{l(l+1)}{r^2}\right]-\frac{\pi}{12r}+\sigma r\right\}U(r)=EU(r) \tag{2.18}$$

or

$$\left[\frac{\mathrm{d}^2}{\mathrm{d}r^2}+\frac{2m}{\hbar^2}\left(E+\frac{\pi}{12r}-\sigma r-\frac{\hbar^2}{2m}\frac{l(l+1)}{r^2}\right)\right]U(r)=0 \tag{2.19}$$

Code was written using the C++ programming language to solve equation (2.19). A `void` function was written to set up the initial potential. The code was edited to read from the command line to allow the selection of a range of different potentials, including the Cornell potential above. Furthermore, the code was made to accept the input of an orbital angular momentum quantum number l_{ang}.

In addition a `void` function was written to use the *Numerov Three-Point-Algorithm* shooting method to numerically integrate for a trial solution energy E from both the left and the right, by specifying the wavefunction $U(r)$ at the end-points and the next-to-end-points. Then by Numerov

$$U_{n+1}(r)=\frac{2(1-\frac{5}{12}l^2k_n^2)U_n(r)-(1+\frac{1}{12}l^2k_{n-1}^2)U_{n-1}(r)}{1+\frac{1}{12}l^2k_{n+1}^2} \tag{2.20}$$

where

$$l=\frac{1}{N-1}$$

is the step size for the discretise spatial variable, N is the number of points, and

$$k_n=\gamma^2[E-V(r_n)]$$

with, for equation (2.19),

$$\gamma^2=\frac{2m}{\hbar^2}$$

The system was solved using zero Dirichlet boundary conditions.

The *Euler Difference* was then used to numerically compute the approximate slope of the function $U(r)$ by

$$U'(r)\simeq\frac{U(r+l)-U(r)}{l} \tag{2.21}$$

and the difference between the left-shooting slope and the right-shooting slope was thus computed.

The process was repeated for a new infinitesimally incremented trail solution energy $E + \delta E$. Next the old-slope and new-slope were compared. Finally, an accept/reject algorithm was written to accept the incremented trail energy, or to reject it in favour of a new trial solution energy with a smaller infinitesimal increment $\delta E' = \delta E/2$.

This process was repeated until the wavefunction was within an acceptable threshold of a real solution.

Another `void` function was added to the code to output the radial wavefunction $R(r)$ so that it may be plotted using *Gnuplot*.

2.3 Further Potential Function Simulations

Code was added to the `.cpp` file to allow for models of the Hydrogen atom radial wavefunctions, where here

$$V(r) = -\frac{e^2}{r} \tag{2.22}$$

where e is the charge on the electron, whence substitution into equation (2.19) yields

$$\left[\frac{\mathrm{d}^2}{\mathrm{d}r^2} + \frac{2m}{\hbar^2}\left(E + \frac{e^2}{r} - \frac{\hbar^2}{2m}\frac{l(l+1)}{r^2}\right)\right] U(r) = 0 \tag{2.23}$$

In addition, a potential function for the Gluon-Flux tube model

$$V(r) = -A\frac{1}{r} + Br^2 \tag{2.24}$$

was added, where A amd B are some constants, to give

$$\left[\frac{\mathrm{d}^2}{\mathrm{d}r^2} + \frac{2m}{\hbar^2}\left(E + A\frac{1}{r} - Br^2 - \frac{\hbar^2}{2m}\frac{l(l+1)}{r^2}\right)\right] U(r) = 0 \tag{2.25}$$

2.4 Results & Analysis

The following graphs of the radial wavefunction $R(r)$ versus the radial distance r for electrons in the Hydrogen Atom potential were plotted

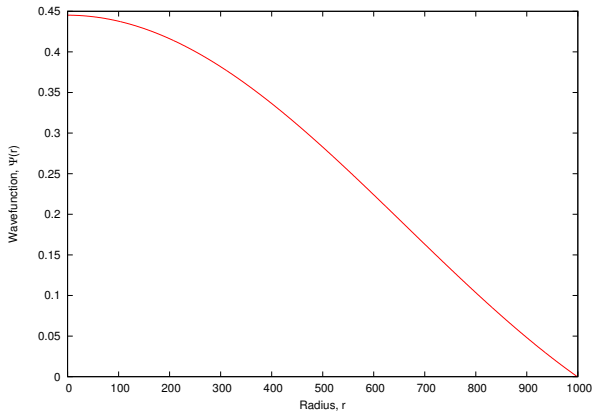

(a) $\ell = 0$ Angular Momentum

Figure 2.1: $n = 1$ States of The Hydrogen Atom

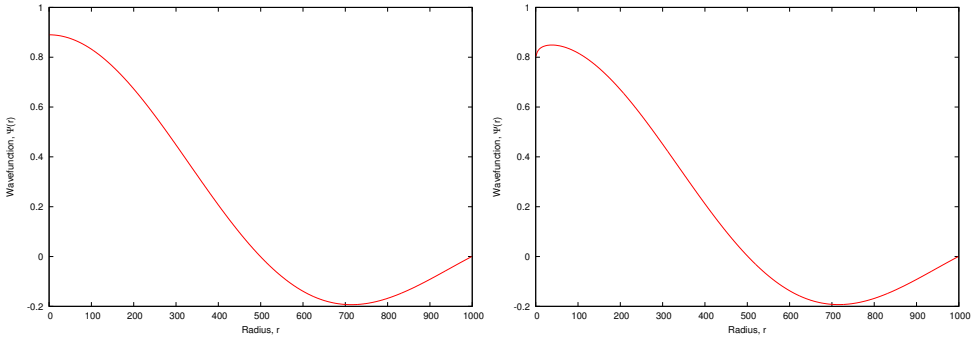

(a) $\ell = 0$ Angular Momentum (b) $\ell = 1$ Angular Momentum

Figure 2.2: $n = 2$ States of The Hydrogen Atom

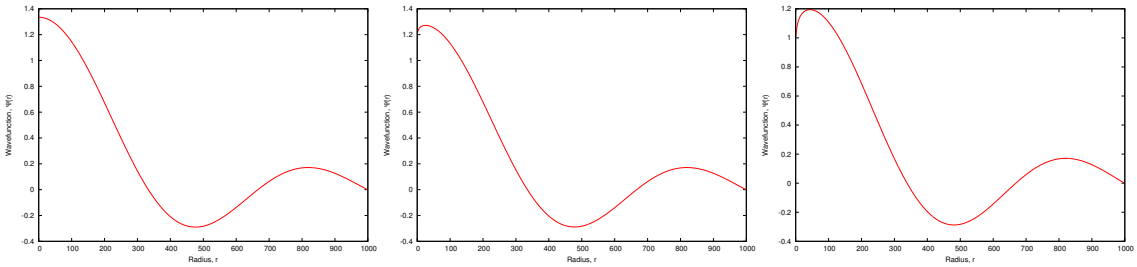

(a) $\ell = 0$ Angular Momentum (b) $\ell = 1$ Angular Momentum (c) $\ell = 2$ Angular Momentum

Figure 2.3: $n = 3$ States of The Hydrogen Atom

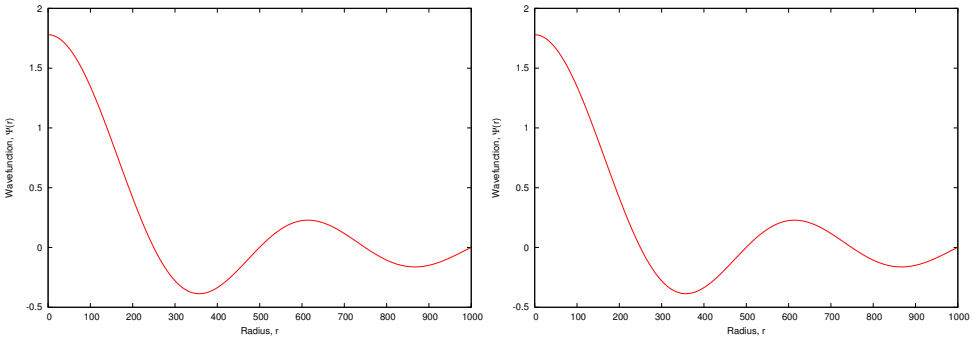

(a) $\ell = 0$ Angular Momentum

(b) $\ell = 1$ Angular Momentum

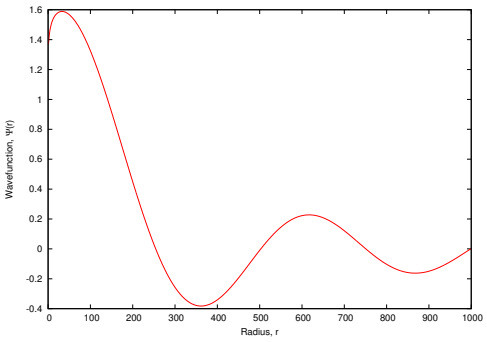

(c) $\ell = 2$ Angular Momentum

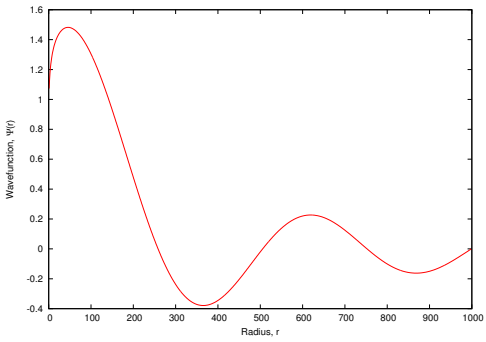

(d) $\ell = 3$ Angular Momentum

Figure 2.4: $n = 4$ States of The Hydrogen Atom

In addition, graphs of the radial wavefunctions for quarks in the Cornell Potential $R(r)$ versus the radial distance r were plotted

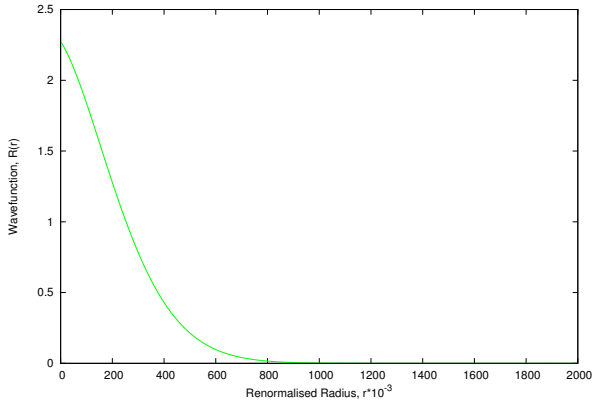

(a) $\ell = 0$ Angular Momentum

Figure 2.5: $n = 1$ States of A Charmonium in The Cornell Potential

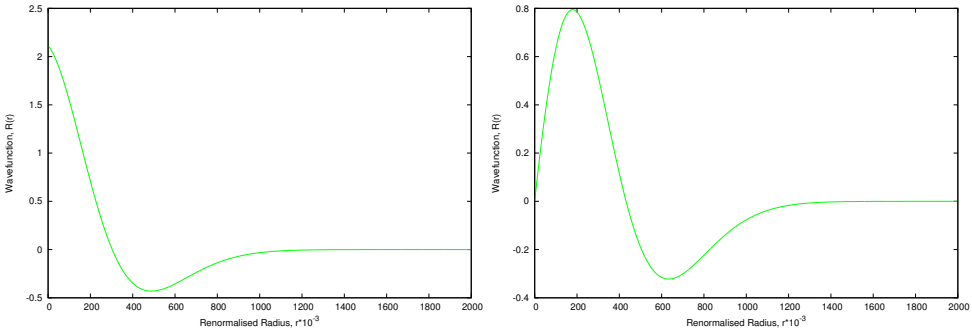

(a) $\ell = 0$ Angular Momentum (b) $\ell = 1$ Angular Momentum

Figure 2.6: $n = 2$ States of A Charmonium in The Cornell Potential

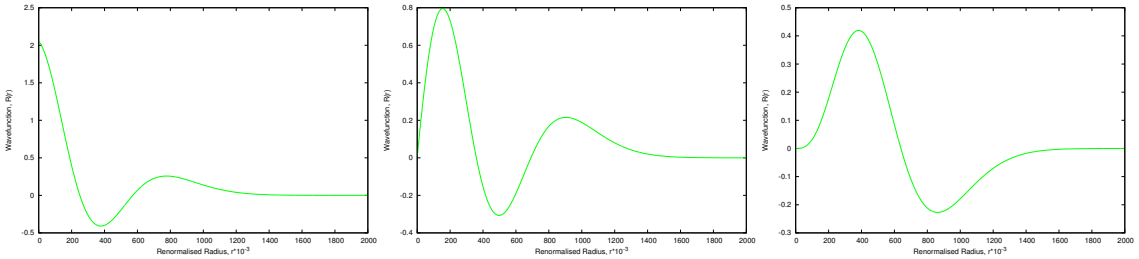

(a) $\ell = 0$ Angular Momentum (b) $\ell = 1$ Angular Momentum (c) $\ell = 2$ Angular Momentum

Figure 2.7: $n = 3$ States of A Charmonium in The Cornell Potential

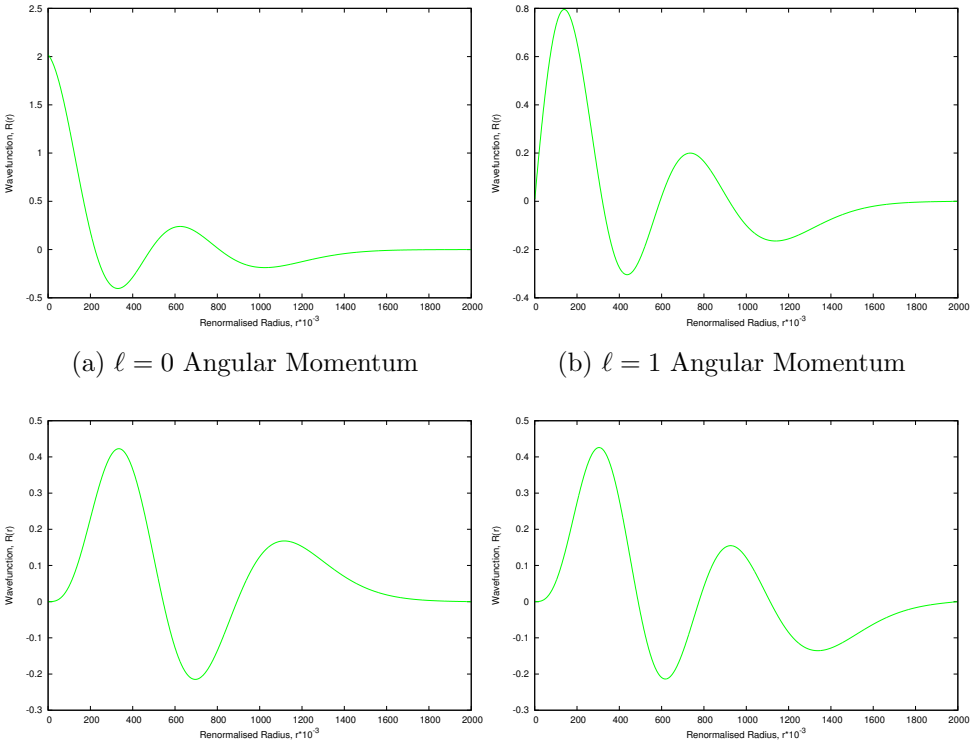

(a) $\ell = 0$ Angular Momentum

(b) $\ell = 1$ Angular Momentum

(c) $\ell = 2$ Angular Momentum

(d) $\ell = 3$ Angular Momentum

Figure 2.8: $n = 4$ States of Charmonium in The Cornell Potential

Finally, the following graphs of the radial wavefunctions for quarks in the potential of the Gluon-Flux Tube Model were plotted

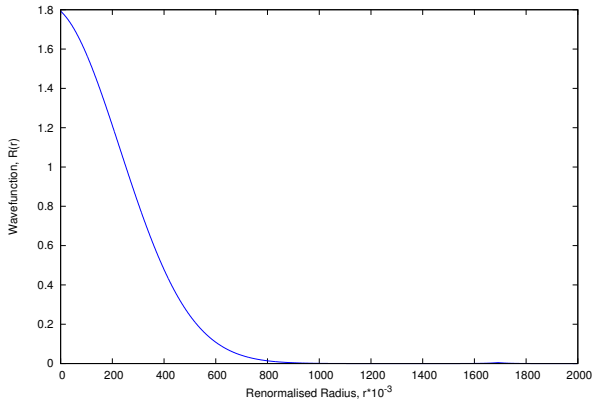

(a) $\ell = 0$ Angular Momentum

Figure 2.9: $n = 1$ States of The Gluon-Flux Tube Model Charmonium

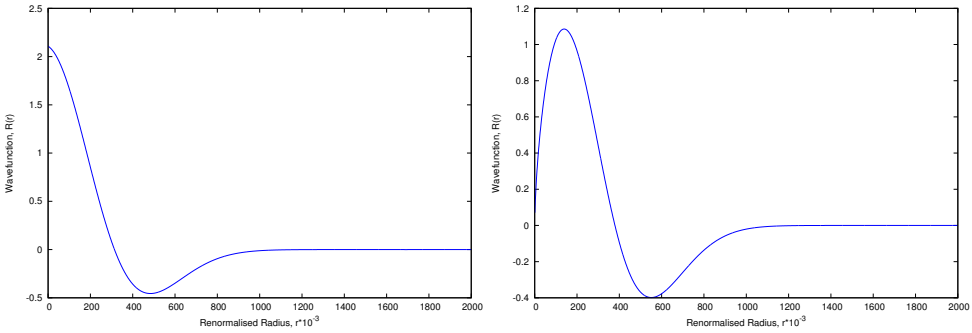

(a) $\ell = 0$ Angular Momentum (b) $\ell = 1$ Angular Momentum

Figure 2.10: $n = 2$ States of The Gluon-Flux Tube Model Charmonium

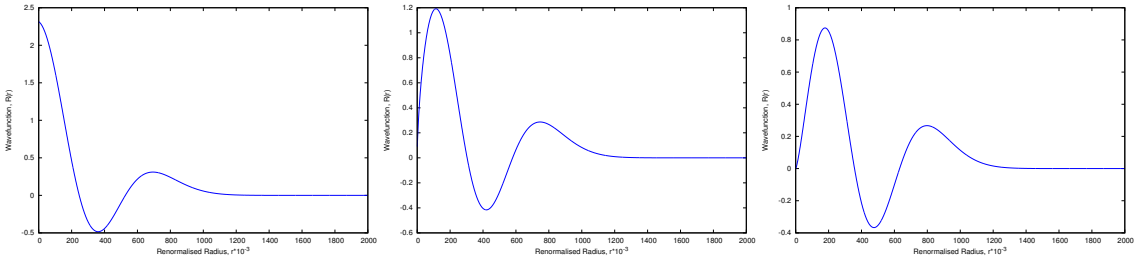

(a) $\ell = 0$ Angular Momentum (b) $\ell = 1$ Angular Momentum (c) $\ell = 2$ Angular Momentum

Figure 2.11: $n = 3$ States of The Gluon-Flux Tube Model Charmonium

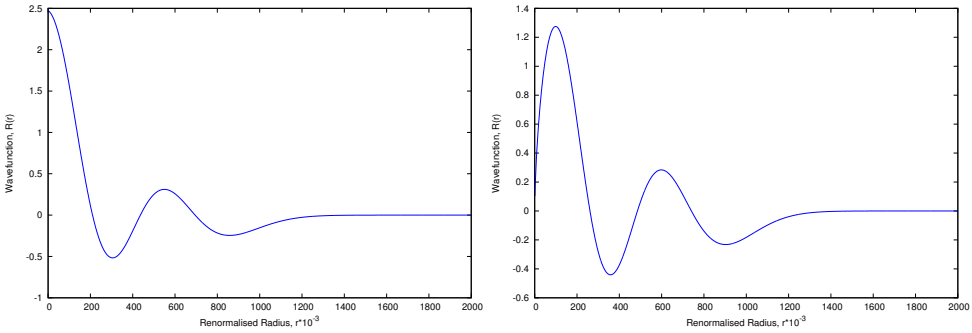

(a) $\ell = 0$ Angular Momentum (b) $\ell = 1$ Angular Momentum

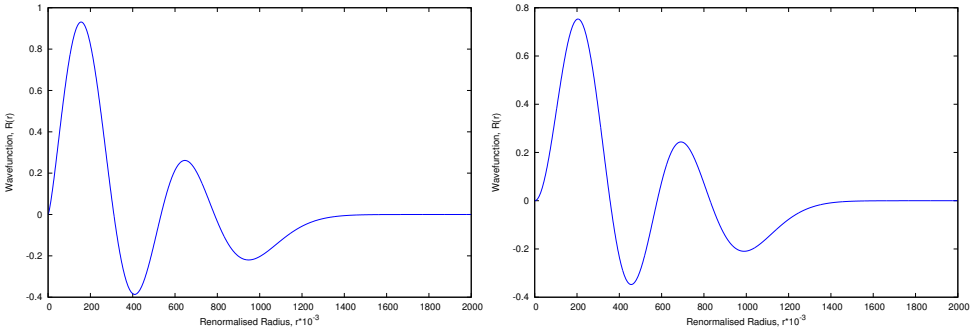

(c) $\ell = 2$ Angular Momentum (d) $\ell = 3$ Angular Momentum

Figure 2.12: $n = 4$ States of The Gluon-Flux Tube Model Charmonium

In addition, a graph of the spectrum of the excitation states of Charmonium as calculated with the Cornell potential was plotted

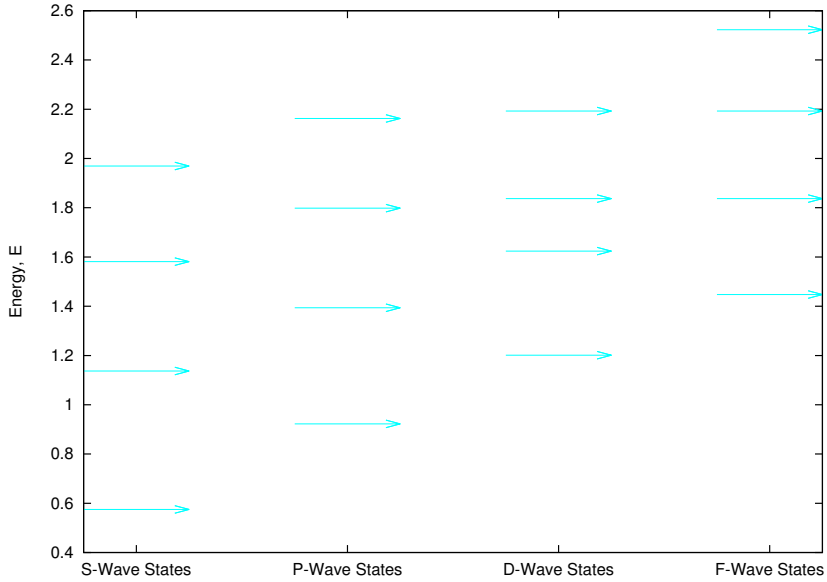

Figure 2.13: Charmonium Excitation States In The Cornell Potential

as was that of the flux-tube potential

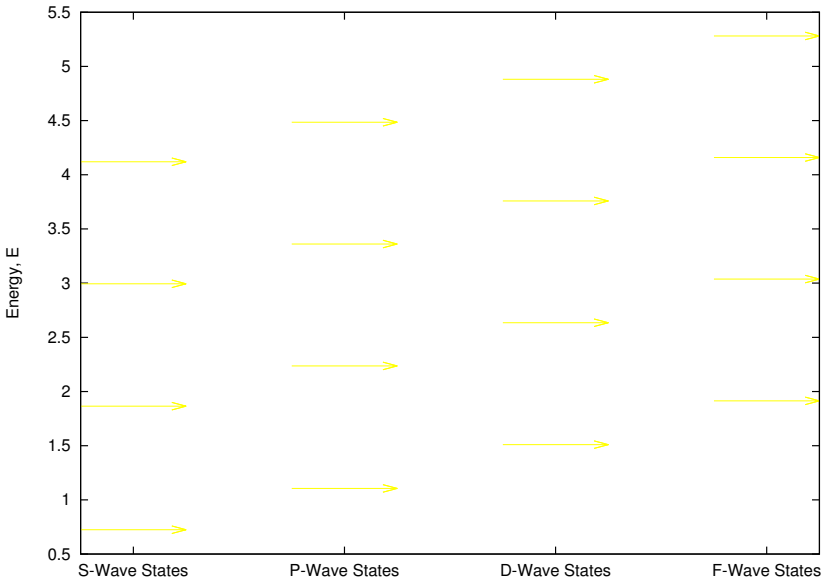

Figure 2.14: Charmonium Excitation States In The Gluon Flux-Tube Potential

Chapter 3

Lattice Charmonium Spectroscopy

3.1 Correlation Function Calculations

A one-dimensional periodic set of quantum fields ϕ_k on the lattice are considered for $k = 0, 1, 2, \ldots, N-1$ with action

$$S = \sum_{k,k'} \phi_k \Box_{k,k'} \phi_{k'} \tag{3.1}$$

where

$$\Box_{k,k'} = m^2 \delta_{k,k'} + (-\delta_{k,k'+1} - \delta_{k,k'-1} + 2\delta_{k,k'}) \tag{3.2}$$

Then the two-point correlation function

$$c(l) = \int_{-\infty}^{\infty} \prod_k \mathrm{d}\phi_k \, \phi_{j+l} \phi_j \exp(-S) \tag{3.3}$$

may be given by

$$c(l) = \frac{1}{Z[0]} \frac{\partial}{\partial J_{j+l}} \frac{\partial}{\partial_j} Z[J] \bigg|_{J=0} \tag{3.4}$$

where

$$Z_0[J] = \int_{-\infty}^{\infty} \mathrm{d}[\phi(x)] \, \exp\left(iS[\phi(x)] + i \int_{-\infty}^{\infty} J(x)\phi(x) \right) \tag{3.5}$$

is the generating functional, with J a source field, or on transforming to Euclidean time $t \to i\tau$

$$Z_0[J] = \int_{-\infty}^{\infty} \mathrm{d}[\phi(x)] \, \exp\left(-S[\phi(x)] + \int_{-\infty}^{\infty} J(x)\phi(x)\right) \tag{3.6}$$

This is simply

$$< 0|\phi_{j+l}\phi_j|0 > \tag{3.7}$$

Here there is nearest neighbour coupling only, whence $k' = k$ gives

$$\Box_{k,k} = m^2 + 2$$

while $k' = k - 1$ gives

$$\Box_{k,k-1} = -1$$

and $k' = k + 1$ gives

$$\Box_{k,k-1} = -1$$

yielding

$$S = \sum_k (m^2 + 2)\phi_k^2 - \phi_k\phi_{k-1} - \phi_k\phi_{k+1} \tag{3.8}$$

Hence the action may be written as a matrix

$$S = \sum_{m,n} \phi_m M_{m,n} \phi_n \tag{3.9}$$

where M is a tri-diagonal symmetric matrix, and invertible if $\det(M) \neq 0$, whence M is solvable, with

$$M = \begin{pmatrix} (m^2+2) & -1 & 0 & 0 & \cdots \\ -1 & (m^2+2) & -1 & 0 & \cdots \\ 0 & -1 & (m^2+2) & -1 & \cdots \\ 0 & 0 & -1 & (m^2+2) & \cdots \\ \vdots & \vdots & \vdots & \vdots & \ddots \end{pmatrix}$$

This gives

$$Z_0[J] = \int_{-\infty}^{\infty} \prod_k \mathrm{d}\phi_k \, \exp\left(\sum_{m,n} \phi_m M_{m,n} \phi_n + \sum_n J_n \phi_n \right) \tag{3.10}$$

Making an orthogonal transformation

$$\tilde{M} = RMR^{-1}$$

where $R^T = R^{-1}$ so that

$$\phi \to \tilde{\phi} = R\phi \quad \text{and} \quad J \to \tilde{J} = RJ$$

yields

$$S = \sum_k \lambda_k \tilde{\phi_k}^2 + \tilde{J}k\tilde{\phi}_k \tag{3.11}$$

where the λ_k are the eigenvalues of M. Here R is an orthogonal transformation and so the measure is invariant such that

$$\prod_k \mathrm{d}\tilde{\phi}_k = \prod_k \mathrm{d}\phi_k$$

Then

$$\begin{aligned} Z_0[J] &= \int_{-\infty}^{\infty} \prod_k \mathrm{d}\tilde{\phi}_k \, \exp\left(-\sum_k \lambda_k \tilde{\phi_k}^2 + \tilde{J}_k \tilde{\phi}_k \right) \\ &= \prod_k \left\{ \int_{-\infty}^{\infty} \mathrm{d}\tilde{\phi}k \, \exp\left(-\lambda_k \tilde{\phi_k}^2 + \tilde{J}_k \tilde{\phi}_k \right) \right\} \end{aligned} \tag{3.12}$$

and this is a Gaussian integral. But for a Gaussian integral

$$\int_{-\infty}^{\infty} \mathrm{d}x \, \exp(-x^2) = \sqrt{\pi} \tag{3.13}$$

and so completing the square

$$-\left(\lambda_k \tilde{\phi_k}^2 - \tilde{J}_k \tilde{\phi}_k\right) = -\left(\sqrt{\lambda_k}\,\tilde{\phi}_k - \frac{\tilde{J}_k}{2\sqrt{\lambda_k}}\right)^2 + \frac{\tilde{J_k}^2}{4\lambda_k} \tag{3.14}$$

gives

$$\begin{aligned} Z_0[J] &= \prod_k \left\{ \int_{-\infty}^{\infty} \mathrm{d}\tilde{\phi_k} \, \exp\left[-\left(\sqrt{\lambda_k}\,\tilde{\phi}_k - \frac{\tilde{J}_k}{2\sqrt{\lambda_k}}\right)^2 + \frac{\tilde{J_k}^2}{4\lambda_k} \right] \right\} \\ &= \prod_k \left\{ \exp\left(\frac{\tilde{J_k}^2}{4\lambda_k}\right) \int_{-\infty}^{\infty} \mathrm{d}\tilde{\phi_k} \, \exp\left[-\left(\sqrt{\lambda_k}\,\tilde{\phi}_k - \frac{\tilde{J}_k}{2\sqrt{\lambda_k}}\right)^2 \right] \right\} \end{aligned} \tag{3.15}$$

Letting

$$\hat{\phi}_k = \sqrt{\lambda_k}\,\tilde{\phi}_k - \frac{\tilde{J}_k}{2\sqrt{\lambda_k}}$$

whence

$$\mathrm{d}\hat{\phi}_k = \sqrt{\lambda}\,\mathrm{d}\tilde{\phi}_k$$

yields

$$\begin{aligned} Z_0[J] &= \prod_k \left\{ \exp\left(\frac{\tilde{J_k}^2}{4\lambda_k}\right) \int_{-\infty}^{\infty} \frac{\mathrm{d}\hat{\phi}_k}{\sqrt{\lambda_k}} \, \exp\left(-\hat{\phi_k}^2\right) \right\} \\ &= \prod_k \frac{1}{\sqrt{\lambda_k}} \exp\left(\frac{\tilde{J_k}^2}{4\lambda_k}\right) \left(\sqrt{\pi}\right) \\ &= \prod_k \sqrt{\frac{\pi}{\lambda_k}} \exp\left(\frac{\tilde{J_k}^2}{4\lambda_k}\right) \end{aligned} \tag{3.16}$$

or

$$Z_0[J] = \sqrt{\frac{\pi}{\det(M)}} \exp\left(1/4 \sum_{k,k'} \tilde{J}_k M^{-1}_{k,k'} \tilde{J}_{k'}\right) \tag{3.17}$$

where in a general basis

$$\prod_k \sqrt{\frac{1}{\lambda_k}} = [\det(M)]^{-1/2} \quad \text{and} \quad \prod_k \exp\left(\frac{\tilde{J_k}^2}{4\lambda_k}\right) = \exp\left(1/4 \sum_{k,k'} \tilde{J}_k M^{-1}_{k,k'} \tilde{J}_{k'}\right)$$

Hence

$$\begin{aligned} c(l) = & \frac{1}{Z[0]} \frac{\partial}{\partial J_{j+l}} \frac{\partial}{\partial_j} \left\{ \sqrt{\frac{\pi}{\det(M)}} \exp\left(1/4 \sum_{k,k'} \tilde{J}_k M^{-1}_{k,k'} \tilde{J}_{k'}\right) \right\} \Bigg|_{J=0} \\ = & \sqrt{\frac{\pi}{\det(M)}} \frac{1}{4} M^{-1}_{j+l,j} \end{aligned} \tag{3.18}$$

It remains to find the eigenvalues, and thus the inverse matrix elements $M^{-1}_{k,k'}$. Well,

$$\sum_\ell M_{k,\ell} M^{-1}_{\ell,k'} = \delta_{k,k'} \tag{3.19}$$

Furthermore, by Fourier

$$f(x) = \frac{1}{\sqrt{\pi}} \int_{-\infty}^{\infty} \tilde{f}(k) \exp(ikx) \mathrm{d}k \tag{3.20}$$

where

$$\tilde{f}(k) = \frac{1}{\sqrt{\pi}} \int_{-\infty}^{\infty} f(x) \exp(-ikx) \mathrm{d}x \tag{3.21}$$

Now, in four dimensions the Dirac-delta function may be written

$$\delta_{k,k'} = \int_{-\infty}^{\infty} \frac{\mathrm{d}^4 p}{(2\pi)^4} \exp[ip(k-k')] \tag{3.22}$$

Thus the matrix M may be written

$$M_{k,k'} = \int_{-\infty}^{\infty} \frac{\mathrm{d}^4 p}{(2\pi)^4} \tilde{M}(p) \exp[ip(k-k')] \tag{3.23}$$

where

$$\begin{aligned} \tilde{M}(p) = & \int_{-\infty}^{\infty} M(k) \exp(-ipk) \mathrm{d}k \\ = & \int_{-\infty}^{\infty} \left[m^2 \delta_{k,k'} + (-\delta_{k,k'+1} - \delta_{k,k'-1} + 2\delta_{k,k'})\right] \exp(-ipk) \mathrm{d}k \end{aligned} \tag{3.24}$$

Then making substitutions for the Dirac-delta functions using equation (3.22) and using the trigonometric identity

$$1 - \cos(p) = \sin^2(p/2)$$

gives

$$\tilde{M(p)} = \frac{1}{(2\pi)^4}\left(m^2 + 4\sin^2(p/2)\right) \tag{3.25}$$

Hence

$$M_{k,k'} = \int_{-\infty}^{\infty} \frac{\mathrm{d}^4 p}{(2\pi)^4}\left(\frac{1}{(2\pi)^4}\left(m^2 + 4\sin^2(p/2)\right)\right)\exp[ip(k-k')] \tag{3.26}$$

Letting

$$M^{-1}_{k,k'} = \int_{-\infty}^{\infty} \frac{\mathrm{d}^4 p}{(2\pi)^4} G(k)\exp[ip(k-k')] \tag{3.27}$$

for some Green function $G(k)$ such that

$$\Box G(k) = \delta(k) \tag{3.28}$$

with

$$\begin{aligned}\sum_{\ell} M_{k,\ell} M^{-1}_{\ell,k'} =&\ \delta_{k,k'} \\ &= \int_{-\infty}^{\infty} \frac{\mathrm{d}^4 p}{(2\pi)^4}\exp[ip(k-k')]\end{aligned} \tag{3.29}$$

or

$$\begin{aligned}\sum_{\ell}\int_{-\infty}^{\infty} \frac{\mathrm{d}^4 p}{(2\pi)^4}\left(\frac{1}{(2\pi)^4}\left(m^2 + 4\sin^2(p/2)\right)\right)\exp[ip(k-\ell)]\int_{-\infty}^{\infty}\frac{\mathrm{d}^4 p'}{(2\pi)^4}G(k)\exp[ip(\ell-k')] \\ = \int_{-\infty}^{\infty}\frac{\mathrm{d}^4 p}{(2\pi)^4}\exp[ip(k-k')]\end{aligned}$$

yields

$$G(k) = (2\pi)^4 \frac{1}{m^2 + 4\sin^2(p/2)} \tag{3.30}$$

whence

$$\begin{aligned} < 0|\phi_{j+l}(x)\phi_j(x)|0 > =& M^{-1}_{j+l,j} \\ &= \int_{-\infty}^{\infty} \mathrm{d}^4 p \, \frac{1}{m^2 + 4\sin^2(p/2)} \exp(ipl) \end{aligned} \tag{3.31}$$

Putting $z = k - k'$ for ease, it is seen that

$$M^{-1}_{k,k'} = \int_{-\infty}^{\infty} \mathrm{d}^3\vec{p} \exp(-i\vec{p}\cdot\vec{z}) \int_{-\infty}^{\infty} \mathrm{d}p^0 \, \frac{1}{m^2 + 4\sin^2(p/2)} \exp(ip^0 z_0) \tag{3.32}$$

Now, this has poles for

$$4\sin^2(p/2) + m^2 = 0 \tag{3.33}$$

whereupon

$$\sin(p/2) = \frac{im}{2} \quad \text{or} \quad \sin(p/2) = \frac{-im}{2} \tag{3.34}$$

or

$$p_+ = 2\sin^{-1}\left(\frac{im}{2}\right) \quad \text{or} \quad p_- = -2\sin^{-1}\left(\frac{im}{2}\right) \tag{3.35}$$

But,

$$\sin(x) = \frac{\exp(ix) - \exp(-ix)}{2i} \qquad \text{and} \qquad \sinh(x) = \frac{\exp(x) - \exp(-x)}{2} \tag{3.36}$$

and so

$$i\sin(ix) = -\sinh(x) \tag{3.37}$$

Hence for p^0 purely imaginary, such that

$$p^0 = 0 + iq \qquad \text{and} \qquad \mathrm{d}p^0 = i\mathrm{d}q$$

equation (3.34) gives

$$-i\sin(iq/2) = \frac{\pm m}{2}$$

or

$$\sinh(q/2) = \frac{\pm m}{2}$$

and so

$$q_+ = 2\sinh^{-1}\Big(\frac{m}{2}\Big) \quad \text{or} \quad q_- = -2\sinh^{-1}\Big(\frac{m}{2}\Big) \tag{3.38}$$

Now, by Cauchy

$$\int_\gamma f(z)\mathrm{d}z = 2\pi i \sum_j n(w_j,\gamma)\mathrm{Res}_{z=w_j} f(z) \tag{3.39}$$

with

$$\begin{aligned}\mathrm{Res}_{z=w_j} f(z) =& \lim_{z\to w_j} (z-w_j)\, f(z) \\ =& \frac{g(w_j)}{h'(w_j)}\end{aligned} \tag{3.40}$$

if

$$f(z) = \frac{g(z)}{h(z)}$$

Here

$$\begin{aligned}\int_\gamma f(q)\mathrm{d}q &= \int_\gamma i\,\mathrm{d}q\, \frac{\exp(-qz_0)}{m^2+4\sin^2(iq/2)} \\ &= \int_\gamma \frac{\mathrm{d}q}{i} \frac{\exp(-qz_0)}{-m^2+4[-i\sin(iq/2)]^2} \\ &= \int_\gamma \frac{\mathrm{d}q}{i} \frac{\exp(-qz_0)}{-m^2+4\sinh^2(q/2)} \qquad \equiv \int_\gamma \frac{g(q)}{h(q)}\mathrm{d}q\end{aligned} \tag{3.41}$$

where

$$g(q) = \exp(-qz_0) \quad \text{and} \quad h(q) = i[-m^2+4\sinh^2(q/2)] \tag{3.42}$$

and thus

$$\begin{aligned}\mathrm{Res}_{q=q_+} f(q) =& \frac{g(q_+)}{h'(q_+)} \\ =& \frac{1}{i} \frac{\exp(-q_+z_0)}{\big(-m^2+4\sinh^2(q/2)\big)'\,|_{q=q_+}} \\ =& \frac{1}{i} \frac{\exp(-q_+z_0)}{(2\sinh(q))\,|_{q=q_+}} \\ =& \frac{1}{i} \frac{\exp(-2\sinh^{-1}(m/2)z_0)}{2\sinh\big(2\sinh^{-1}(m/2)\big)}\end{aligned} \tag{3.43}$$

Choosing a path γ in the right half-plane such that the winding number about q_+ is one, while that of q_- is zero yields

$$\begin{aligned}\int_\gamma f(q)\mathrm{d}q &= 2\pi i \left\{ (1) \left(\frac{1}{i} \frac{\exp(-2\sinh^{-1}(m/2)z_0)}{2\sinh\left(2\sinh^{-1}(m/2)\right)} \right) + (0) \right\} \\ &= \frac{\pi}{\sinh\left(2\sinh^{-1}(m/2)\right)} \exp(-2\sinh^{-1}(m/2)z_0) \end{aligned} \tag{3.44}$$

or

$$\int_\gamma f(q)\mathrm{d}q \equiv C(m)\exp(-2\sinh^{-1}(m/2)z_0) \tag{3.45}$$

with

$$C(m) = \frac{\pi}{\sinh\left(2\sinh^{-1}(m/2)\right)}$$

But $z_0 = k_0 - k_0'$ is the time separation, and so it is found that the two-point correlator is an exponential function of the mass of the particle m, and the time separation such that

$$< 0|\phi_k(x)\phi_{k'}(x)|0 > = M^{-1}_{k,k'} = C(m)\exp[-2\sinh^{-1}(m/2)(k_0 - k_0')] \tag{3.46}$$

Thus it is seen that the two-point correlation function for a quantum chromodynamical process falls off exponentially in time with the mass of the particle.

3.2 Monte Carlo Simulations

From above the two-point correlation function is

$$C_{ij}(t_1) = < 0|\Phi_i(t_1)\Phi_j^\dagger(0)|0 > \tag{3.47}$$

where the Φ_i are operators of Dirac spinors and the Dirac matrices such that

$$\Phi_k = \sum_x \bar{c}^\alpha(x)\gamma_k^{\alpha\beta}c^\beta(x) \qquad \text{or} \qquad \Phi_\ell = \sum_x \bar{c}^\alpha(x)\gamma_\ell^{\alpha\beta}(\mathcal{D}_m\mathcal{D}_n + \mathcal{D}_n\mathcal{D}_m)c^\beta(x)$$

say. Taking a Euclidean transformation $t \to -i\tau$ the Heisenberg operator picture yields

$$\begin{aligned} C_{ij}(t_1) &= <0|\exp(\mathcal{H}t_1)\Phi_i(t_1)\exp(-\mathcal{H}t_1)\exp[\mathcal{H}\cdot(0)]\Phi_j^\dagger(0)\exp[-\mathcal{H}\cdot(0)]|0> \\ &= <0|\Phi_i(t_1)\exp(-\mathcal{H}t_1)\Phi_j^\dagger(0)|0> \end{aligned} \tag{3.48}$$

Then on inserting a complete set of states $|n><n|$ it is seen that

$$\begin{aligned} C_{ij}(t_1) &= \sum_n <0|\Phi_i(t_1)\exp(-\mathcal{H}t_1)|n><n|\Phi_j^\dagger(0)|0> \\ &= \sum_n <0|\Phi_i(t_1)|n><n|\Phi_j^\dagger(0)|0>\exp(-E_n t_1) \\ &= \sum_n Z_{in}Z_{nj}^*\exp(-E_n t_1) \end{aligned} \tag{3.49}$$

where

$$Z_{in} = <0|\Phi_i(t_1)|n> \qquad \text{and} \qquad Z_{nj}^* = <n|\Phi_j^\dagger(0)|0> \tag{3.50}$$

On the lattice this exponential becomes

$$\exp(-E_n t_1) \;\to\; \exp\left(-(E_n a_t)\frac{t_1}{a_t}\right) \tag{3.51}$$

where a_t is the lattice spacing. Thus the the two-point correlation function equation becomes a generalised eigenvalue problem

$$C_{ij}(t_1) = \lambda_n(t_0,t_1)C(t_o)\vec{v_n} \tag{3.52}$$

where $\lambda_n(t_0,t_1)$ is the generalised eigenvalue with

$$\lambda_n(t_0,t_1) \;\propto\; \exp[-E_n(t_1-t_0)] \tag{3.53}$$

However this is only true in the limit as

$$t_1 - t_0 \to \infty$$

which is not always the case.

For a large enough time separation $t_1 - t_0$ equation (3.53) can be taken to hold. Then, fitting to an exponential decay gives the ground state energy E_1. Furthermore, for a large set of operators $\Psi_i(t)$ the excited state energies can also be computed[86].

A fit to the randomly generated data $\bar{C_{ij}}(t_1 - t_0)$ must be calculated for the correlation functions for a given set of Quantum Chromodynamics operators. This is done by performing a *Chi-Squared Test*. Here

$$\chi^2 = \sum_{i,j,n,t_0} \frac{\left(\bar{C_{ij}}(t_1 - t_0) - C_{ij}(E_n, Z_{in}, Z_{nj}, t_0 - t_1)\right)^2}{\sigma_{ij}^2} \tag{3.54}$$

where σ_{ij}^2 is the variance in the randomly generated Monte Carlo data. This must be minimised with respect to $\{E_n\}$ and $\{Z_{ij}\}$ for a global minimum such that

$$\begin{aligned} \frac{\partial \chi^2}{\partial E_0} = \frac{\partial \chi^2}{\partial E_1} = \cdots = 0 \\ \frac{\partial \chi^2}{\partial Z_{11}} = \frac{\partial \chi^2}{\partial Z_{12}} = \cdots = \frac{\partial \chi^2}{\partial Z_{21}} = \frac{\partial \chi^2}{\partial Z_{22}} = \cdots = 0 \end{aligned} \tag{3.55}$$

Then, if

$$\chi^2 \simeq n \tag{3.56}$$

the fit is within one standard deviation of the Monte Carlo data, and the energy spectrum may be confidently extracted.

3.3 Variational Data Fitting

The `variational_fitter` code was run to fit exponential decaying curves to a range of sets of operators from the T_1^{--} and T_1^{-+} symmetry point groups.

The two ρ operators of the T_1^{-+} group were fitted for correlation times of $4 \leq t_0 \leq 17$. This was followed by fitting the remaining sixteen operators of the T_1^{-+} group for correlation times of $4 \leq t_0 \leq 14$. Finally, all eighteen operators of the T_1^{-+} group were fitted simultaneously for $3 \leq t_0 \leq 15$.

In addition, both the eight ρ and the eight ρ along with the two π operators of

the T_1^{--} group were analysed using the `variational_fitter` code for correlation times of $4 \leq t_0 \leq 14$ and $3 \leq t_0 \leq 15$ respectively. The code was also run to fit all twenty-six operators of the T_1^{--} group simultaneously.

Masses were then extracted from that data which had an acceptable χ^2 value. The scale is set by using the fitting the Ω^{--} meson mass times the lattice constant to the value quoted in the particle data group[87], which gives a value of the lattice constant of $a_t^{-1} = 5.667\,\text{GeV}$.

3.4 Results & Analysis

The Monte Carlo data was found to fit with the theoretical values for the two ρ operators of the T_1^{-+} symmetry point group with acceptable χ^2 values for Euclidean time separations $12 \leq t \leq 17$. This corresponded to a mass of $4.235 \pm 0.011\,\text{GeV}$ where the fitting was performed over the range $5 \leq t_{\text{min / max}} \leq 18$.

Furthermore the data was successfully fitted for the sixteen remaining operators of the T_1^{-+} group with acceptable χ^2 values for Euclidean time separations $9 \leq t \leq 13$. In this case this corresponded to a mass parameter of $4.239 \pm 0.026\,\text{GeV}$ where the fitting was performed over the range $8 \leq t_{\text{min / max}} \leq 18$.

Finally, for all eighteen operators of the T_1^{-+} group the variational fitting was successful with $\chi^2 \simeq n$ for time separations of $9 \leq t \leq 15$. This may be interpreted as a particle with mass $4.211 \pm 0.011\,\text{GeV}$ where the fitting was performed over the range $5 \leq t_{\text{min / max}} \leq 18$.

Thus it is clear that the two ρ operators give the greatest contributions to the physical state of the T_1^{-+} group as the the fitting starts for an earlier range of timeslices than that of the other sixteen operators of the group. This in turn allows for the extraction of a mass parameter with the smallest error range, as the signal to noise ratio is greatest for earlier timeslices.

From the variational fitting performed with the T_1^{--} symmetry point group operators it was found that χ^2 was not within the acceptable range for any time separations for the eight ρ and the eight ρ plus the two π operators. Hence it is seen that there are no gluonic states in the T_1^{--} symmetry point group.

However, the data was found to fit with that of all twenty-six operators of

the T_1^{--} symmetry group for time separations of $11 \leq t \leq 13$. This implies that a particle with a mass of $3.04499 \pm 0.0004\,\mathrm{GeV}$ exists and that the T_1^{--} does indeed have physical states.

Table 3.1: Values for m_0 of the T_1^{-+} Symmetry Point Group

	Both ρ Operators	Remaining 16 Operators	All 18 Operators
First Good Timeslice	0.7473 ± 0.002	0.7480 ± 0.0046	0.743 ± 0.002
	$\simeq 4.235 \pm 0.011\,\mathrm{Gev}$	$\simeq 4.239 \pm 0.026\,\mathrm{Gev}$	$\simeq 4.211 \pm 0.011\,\mathrm{GeV}$
Largest Time Separation	(all the same separation)	(all the same separation)	0.748 ± 0.002
	(with $5 \leq t_{\mathrm{min\,/\,max}} \leq 18$)	(with $8 \leq t_{\mathrm{min\,/\,max}} \leq 18$)	$\simeq 4.239 \pm 0.011\,\mathrm{GeV}$
Smallest χ^2	0.7472 ± 0.0023	0.7491 ± 0.0042	0.742 ± 0.003
	$\simeq 4.234 \pm 0.013\,\mathrm{Gev}$	$\simeq 4.245 \pm 0.024\,\mathrm{GeV}$	$\simeq 4.205 \pm 0.017\,\mathrm{GeV}$

Here the average over all time slices is done over all those time slices for which $\chi^2 \simeq n$ where n is the number of operators.

Chapter 4

Conclusions

4.1 Numerical Calculations of The Radial Wavefunction

It is possible to solve the partial differential Schrödinger equation for the radial wavefunction $R(r)$ using the method of separation of variables. Three equations are obtained for the radial wavefunction $R(r)$ and the angular wavefunctions $\Phi(\phi)$ and $\Theta(\theta)$, though it is customary to combine the angular wavefunctions to give $Y_l^{m_l}(\theta, \phi)$.

Using C++ code to implement the Numerov algorithm it was seen that the radial wavefunction equation could effectively be solved for a range of potential functions, including the Cornell Potential and that of the gluon-flux tube. A $\sqrt{\sigma}$ value of 400 MeV was used to reproduce the linear interaction term.

Graphs of the radial wavefunctions were then plotted for a range of energy levels n and angular momentum quantum numbers l. It was found that the linear term in the Cornell and flux-tube potentials caused the wavefunctions to drop off quickly with increasing r. This is representative of the confinement property of Quantum Chromodynamics.

4.2 Lattice Charmonium Spectroscopy

The path integral formalism is an effective approach to study quantum field theories such as Quantum Chromodynamics. It not only allows for the analytic calculation of correlation functions due to the clear relationship it describes between them and the $\mathcal{L}$agrangian functional, but also the possibility to put a quantum field theory on a regular lattice in a well defined manor.

The analytic calculation of correlation functions is complicated to begin with. Putting a quantum field theory on a lattice then, such as with lattice Quantum Chromodynamics, introduces new complications. However it still possible to compute such functions analytically using the Fourier transform representation and the Green function method. For a lattice quantum field theory it is found that the two-point correlation functions decay exponentially in Euclidean time with the mass of the state.

This allows for the variational fitting of a curve to a data array and for the extraction of a mass parameter by the chi-squared test method. For the data set analysed under the T_1^{--} and T_1^{-+} symmetry point groups physical states with masses of $3.04499 \pm 0.0004\,\text{GeV}$ and $4.211 \pm 0.011\,\text{GeV}$ respectively were found.

In the case of the operators of the T_1^{-+} group if was seen that the two ρ operators give the majority of the contribution to the sate, as they gave rise to the earliest variational fitting of the data. This corresponds to an exotic $c\bar{c}$ state, as these second-derivative operators give contributions from the gluons.

4.3 Prospects of Lattice Quantum Chromodynamics

The lattice allows for the non-perturbative study of Quantum Chromodynamics. Though it introduces problems such as fermion doubling, and systematic errors due to both the lattice spacing and the finite volume of space-time over which the simulations are performed, as well as statistical errors due to the nature of Monte Carlo integration, these can be effectively overcome with novel ideas such as those of the staggered fermion and the powerful machines of the UKQCD collaboration to employ larger lattices and sampling sizes.

Lattice Quantum Chromodynamics has produced better and better predictions of the hadronic spectrum. *ab inito* calculation of the proton mass has always been an acid test for Quantum Chromodynamics. Increasingly accurate mass parameters for the quarks have been computed from the measurable properties of hadrons[88, 89]. As well as these, the strong coupling parameter α_s has been measured to increasing accuracy, with a current value with respect to the M_Z scale of $\alpha_s(M_Z) = 0.1183 \pm 0.0008$[90]. This is in excellent agreement with the experimentally measured value of $\alpha_s = 0.1186 \pm 0.0011$ calculated as an average from high energy scattering experiments and decays[91]. As well as this lattice Quantum Chromodynamics allows for the study of exotic mesonic states and purely gluonic states as discussed extensively above (see 1.9).

Calculations show that the interaction energy increases linearly with quark separation[92]. However the continuum limit of any lattice calculation must be taken before conclusions may be made. Unfortunately asymptotic freedom starts to take effect at smaller quark separations. Simulations suggest that as the lattice spacing tends towards zero confinement holds, however it remains to prove that confinement holds at zero lattice spacing.

It is believed that it is possible to have free quarks and antiquarks given certain conditions of high energy and pressure in which quarks and gluons can condense into a plasma state[93]. Here, the idea of individual hadrons is meaningless, and the system consists of free quarks and gluons, the overall system being in a colour singlet state. In a similar manner to that of the Mott insulator-metal phase transition, the gluons act to screen the colour force between the high density quarks, allowing the flow of colour charge. Lattice Quantum Chromodynamics simulations suggest that the *Deconfinement Transition* should occur at temperatures of about $10^{12}K$ and densities about 10 times that of normal nuclei[94]. Demonstrations of deconfinement, that is, the *Quark-Gluon Plasma* are made possible using lattice Quantum Chromodynamics.

Quantum Chromodynamics is an extremely interesting theory, with a huge number of research opportunities to offer. The chiral symmetry of Quantum Chromodynamics[95], whose breaking can give rise to the small mass of the pions[96, 97, 98], may be recovered above the *Chiral Restoration Phase Transition*. Modern simulations have helped to show that Quantum Chromodynamics

predicts this transition[99, 100, 101]. Other active areas of research are *Quark Cooper Pairs*, *Colour Superconductivity* and *Colour-Flavour Locking*[102, 103]. There is not yet any lattice non-perturbative simulations that suggest these properties conclusively, but rather they remain to be explored. Another open question is that of the coincidental cancellation of the CP violating term in the Quantum Chromodynamics $\mathcal{L}$agrangian, known as the *Strong CP Problem*[104].

Even the fields of astrophysics and cosmology are united with Quantum Chromodynamics in this front, with the prediction of the axion[105, 106] to resolve the strong CP problem playing the rôle of a dark matter candidate, as well as the possibility of *Neutron Stars* being a physical state of the quark-gluon plasma[107]. These and many other avenues of exploration await lattice Quantum Chromodynamics for a complete description.

4.4 Future Work

The general method of implementing C++ code to numerically solve the radial schrödinger equation has herein been established. To accurately reproduce the charmonium spectrum will require further fine tuning and optimisation of this code. It is hoped that the spectrum can be reproduced to show the correct scaling between the different energy levels upon fixing the 1S–1P splitting. More work on this will have to be done if an accurate investigation is to be carried out.

From the results generated in this study and the methods used therein, the investigation of a wide range of exotic charmonium mesonic states may follow directly using the `variational_fitter` code to preform chi-squared tests of the multitude of data available. With the extraction of more mass parameters of more states an increasing number of exotic states can potentially be identified as physical states of the $c\bar{c}$ system.

Furthermore, it remains to use the `variational_fitter` code to preform chi-squared testing analysis of the data generated using the `CUDA LQCD Correlator Calculator` software recently developed by Ó Conbhuí[108]. This software is capable of calculating the correlation functions of quantum fields in an extremely computationally inexpensive fashion. Thus, more data may become available, with the prospect of predicting new mesonic states.

References

[1] I. Newton, Philosophiae Naturalis Principia Mathematica (1687).

[2] A. Einstein, Jahrbuch der Radioaktivitaet und Elektronik **4**, 411 (1907).

[3] A. Einstein, Sitzungsberichte der Preussischen Akademie der Wissenschaften zu Berlin, 844 (1915).

[4] A. Einstein, Sitzungsberichte der Preuischen Akademie der Wissenschaften, 142 (1917).

[5] E. Fermi, Ricerca Scientifica **4**, 491 (1933).

[6] S. L. Glashow, Nuclear Physics **22**, 579 (1961).

[7] S. Weinberg, Physical Review Letters **19**, 1264 (1967).

[8] A. Salam, Elementary Particle Physics (ed. N. Svartholm) 367 (Almqvist and Wiksills, Stockholm) (1968).

[9] G. t'Hooft, Nuclear Physics B **33**, 173 (1971), and **35**, 167 (1971).

[10] M. Gell-Mann and Y. Neeman, The Eightfold Way (Benjamin, New York) (1964).

[11] M. Gell-Mann, Physics Letters **8**, 214 (1964).

[12] G. Zweig, CERN Rep. 8182/TH.401, 8419/TH.412.

[13] J. J. Aubert *et al.*, Physical Review Letters **33**, 1404 (1974).

[14] J.-E. Augustin *et al.*, Physical Review Letters **33**, 1406 (1974).

[15] S. L. Glashow, J. Iliopoulos and L. Maiani, Physical Review D **2**, 1585 (1970).

[16] R. P. Feynman, Physical Review Letters **23**, 1415 (1969).

[17] H. Kendall, Proceedings of the Fifth International Symposium on Electron and Photon Interactions at High Energy, Cornell University (1971).

[18] O. W. Greenberg, American Journal of Physics **50**, 1074 (1982).

[19] C. N. Yang and R. L. Mills, Physical Review **96**, 191 (1954).

[20] O. W. Greenberg, Physical Review Letters **13**, 589 (1964).

[21] O. W. Greenberg and C. A. Nelson, Physics Reports **32C**, 69 (1977).

[22] H. D. Politzer, Physical Review Letters **30**, 1346 (1973).

[23] D. Gross and F. Wilczek, Physical Review Letters **30**, 1343 (1973).

[24] J. D. Bjorken, Physical Review **179**, 1547 (1969).

[25] S. Coleman and D. Gross, Physical Review Letters **31**, 1343 (1973).

[26] H. Fritzsch, M. Gell-Mann and H. Leutwyler, Physics Letters **47 B**, 365 (1973).

[27] K. G. Wilson, Physical Review D **10**, 2445 (1974).

[28] K. G. Wilson, Nuclear Physics B, Proceedings Supplements **140**, 3 (2005).

[29] K. Symanzik, Nuclear Physics B **226**, 187 (1983).

[30] K. Symanzik, Nuclear Physics B **226**, 205 (1983).

[31] H. B. Nielson and M. Ninomiya, Nuclear Physics **185**, 20 (1981).

[32] K. G. Wilson, New Phenomena in Subnuclear Physics (ed. A. Zichichi) (Plenum, New York) (1975).

[33] J. B. Kogut and L. Susskind, Physical Review D **11**, 395 (1975).

[34] L. Susskind, Physical Review D **20**, 2610 (1977).

[35] T. Banks, D. R. T. Jones, J. Kogut, S. Raby, P. N. Scharbach, D. K. Sinclair and L. Susskind, Physical Review D **15**, 1111 (1977).

[36] H. Kluberg-Stern, A. Morley O. Napoly and B. Petersson, Nuclear Physics B **220**, 337 (1983).

[37] H. Hamber and G. Parisi, Physical Review Letters **47**, 1792 (1981).

[38] D. H. Weingarten and D. N. Petcher, Physics Letters B **99**, 333 (1981).

[39] R. Burkhaltera *et al.* (CP-PACS Collaboration), Nuclear Physics B - Proceedings Supplements **73**, 3 (1999).

[40] R. Mawhinney, Parallel Computing **25**, 1281 (1999).

[41] C. Allton, Computer Physics Communications **142**, 168 (2001).

[42] C. M. Richards, A. C. Irving, E. B. Gregory and C. McNeile (UKQCD Collaboration), Physical Review D **82**, 034501 (2010).

[43] C. J. Morningstar and M. J. Peardon, Physical Review D **60**, 034509 (1999).

[44] J. Sexton, A. Vaccarino and D. Weingarten, Physical Review Letters **75**, 4563 (1995).

[45] R. P. Feynman, Review of Modern Physics **20**, 367 (1948).

[46] E. Eichten and F. Feinberg, Physical Review Letters **43**, 1205 (1979).

[47] E. Eichten and F. Feinberg, Physical Review D **23**, 2724 (1979).

[48] T. Appelquist and H. D. Politzer, Physical Review Letters **34**, 43 (1975).

[49] T. Appelquist and H. D. Politzer, Physical Review D **12**, 1404 (1975).

[50] E. D. Bloom and G. J. Feldman, Scientific American **5** 66 (1982).

[51] S. Okubo, Physical Letters **5**, 165 (1963).

[52] G. Zweig, CERN Preprints TH, 401 (1964).

[53] G. Zweig, CERN Preprints TH, 412 (1964).

[54] J. Iizuka, Progress in Physics Supplement **37**, 21 (1966).

[55] E. Eichten and K. Gottfried, Physics Letters B **66**, 286 (1977).

[56] J. Conway *et al.*, European Journal of Physics **22**, 533 (2001).

[57] H. R. Quinn and M. S. Witherell, Scientific American **10**, 76 (1998).

[58] A. B. Carter and A. I. Sanda, Physical Review D **23**, 1567 (1981).

[59] D. H. Perkins, Introduction to High-Energy Physics (Addison-Wesley, Massachusetts) 99 (1982).

[60] S. K. Choi *et al.* (Belle Collaboration), Physical Review Letters **91**, 262001 (2003).

[61] B. Aubert *et al.* (BABAR Collaboration), Physical Review D **77**, 111101 (2008).

[62] D. E. Acosta *et al.* (CDF II Collaboration), Physical Review Letters **93**, 072001 (2004).

[63] A. Abulencia *et al.* (CDF Collaboration), Physical Review Letters **98**, 132002 (2007).

[64] T. Aaltonen *et al.* (CDF Collaboration), Physical Review Letters **103**, 152001 (2009).

[65] V. M. Abazov *et al.* (DØ Collaboration), Physical Review Letters **93**, 162002 (2004).

[66] B. Aubert *et al.* (BABAR Collaboration), Physical Review D **77**, 011102 (2008).

[67] T. Aushev *et al.* (Belle Collaboration), Physical Review D **81**, 031103 (2010).

[68] B. Aubert *et al.* (BABAR Collaboration), Physical Review Letters **95**, 142001 (2005).

[69] B. Aubert *et al.* (BABAR Collaboration), arXiv:0808.1543v2 (2008).

[70] Q. He *et al.* (CLEO Collaboration), Physical Review D **74**, 091104 (2006).

[71] C. Z. Yuan *et al.* (Belle Collaboration), Physical Review Letters **99**, 182004 (2007).

[72] B. Aubert *et al.* (BABAR Collaboration), Physical Review Letters **98**, 212001 (2007).

[73] X. L. Wang *et al.* (Belle Collaboration), Physical Review Letters **99**, 142002 (2007).

[74] S. K. Choi *et al.* (Belle Collaboration), Physical Review Letters **100**, 142001 (2008).

[75] N. Brambilla, S. Eidelman, B. K. Heltsley, R. Vogt, G. T. Bodwin, E. Eichten, A. D. Frawley, A. B. Meyer, R. E. Mitchell, V. Papadimitriou, P. Petreczky, A. A. Petrov, P. Robbe, A. Vairo, A. Andronic *et al.*, European Physics Journal C **71**, 1534 (2011).

[76] M. Goldhaber, L. Grodzins, and A. W. Sunyar, Physical Review **109**, 1015 (1958).

[77] B. Aubert et al., Proceedings of the Seventeenth International Conference on High Energy Physics, London (1974).

[78] A. Watson, The Quantum Quark (Cambridge Univeristy Press, Cambridge) (2004).

[79] A. Chodos, R. L. Jaffe, K. Johnson, C. B. Thorn and V. F. Weisskopf, Physical Review D **9**, 3471 (1974).

[80] P. Hasenfratz and J. Kuti, Physics Reports **40 C**, 75 (1978).

[81] T. DeGrand, R. L. Jaffe, K. Johnson and J. Kiskis, Physical Review D **12**, 2060 (1975).

[82] R. L. Jaffe and K. Johnson, Physics Letters **60B**, 201 (1976).

[83] J. F. Donoghue, K. Johnson and B. A. Li, Physical Letters **99B**, 416 (1981).

[84] N. Isgur and J. Paton, Physical Review D **31**, 11 (1985).

[85] W. Marciano and H. Pagels, Nature **279**, 497 (1979).

[86] A. S. Kronfeld, Annual Review of Nuclear Particle and Particle Science **62** (2012).

[87] K. Nakamura *et al.* (Particle Data Group), Journal of Physics G **37**, 075021 (2010).

[88] A. Bazavov *et al.*, Review of Modern Physics **82**, 1349 (2010).

[89] C. McNeile, C. T. H. Davies, E. Follana, K. Hornbostel and G. P. Lepage, Physical Review D **82**, 034512 (2010).

[90] C. T. H. Davies *et al.*, Physical Review D **78**, 114507 (2008).

[91] S. Bethke, The European Physics Journal C **64**, 689 (2009).

[92] R. Sommer, Nuclear Physics B **291**, 673 (1987).

[93] H. Bhor and N. B. Bielsen, Nuclear Physics B **128** 275 (1977).

[94] A. Bazavov *et al.*, Physical Review D **80**, 014504 (2009).

[95] S. Weinberg, Physical Review Letters **18**, 188 (1967).

[96] Y. Nambu, Physical Review Letters **4**, 380 (1960).

[97] J. Goldstone, Nuvov Cimento **19**, 154 (1961).

[98] J. Goldstone, A. Salam and S. Weinberg, Physical Review **127**, 965 (1962).

[99] T. DeGrand, Z. Liu and S. Schaefer, Physical Review D **74**, 094504 (2006).

[100] H. Fukaya *et al.* (JLQCD Collaboration), Physical Review Letters **104**, 122002 (2010).

[101] H. Fukaya *et al.* (JLQCD Collaboration), Physical Review D **83**, 074501 (2011).

[102] M. G. Alford, K. Rajagopal, T. Schaefer and A. Schmitt, Rev of Modern Phys **80**, 1455 (2008).

[103] M. Alford, K. Rajagopal and F. Wilczek, Physics Letters B **422**, 247 (1998).

[104] J. E. Kim and G. Carosi, Review of Modern Physics **82** 557 (2010).

[105] R. D. Peccei and H. R. Quinn, Physical Review Letters **38**, 1440 (1977).

[106] R. D. Peccei and H. R. Quinn, Physical Review D **16**, 6 (1977).

[107] L. Levkova, High Energy Physics - Lattice, arXiv:1201.1516v2 (2012).

[108] P. Ó Conbhuí and M. J. Peardon, Computing Two-Point Correlator Functions On Graphics Processor Units (2012).